SECTION 5: LONG TERM ANALYSIS OF DILUTION OF CONCENTRATED SEA WATER

5) Long-Term Analysis of Dilution of Concentrated Sea Water

In this section we perform modeling simulations on the entire set of 7,523 daily combinations of the 7 controlling variables presented in Figures 3.23 and 3.24 for the period of record from 1980 through mid-2000. This period was selected because it is the longest length of time for which an uninterrupted record of directional wave data can be assembled in this region. The purpose of this long-term continuous modeling exercise was to both establish the viability of the event analysis presented in Section 4 for characterizing low flow and average case, as well as exploring the persistence of all the intermediate outcomes occurring between low flow and average cases. In addition changes to the dispersion statistics of the hyper-saline plume are examined for cold water discharges from AES Huntington Beach, as a consequence of the generating station pumping seawater with a $\Delta T = 0$.

The marine environment around the AES Huntington Beach Generating station has both short-term and long-term variability due to an interplay between climatic variability and certain local features due to physical setting and generating station operations. El Niño events cause significant warming and stratification of the coastal ocean around AES Huntington Beach over recurrence periods of 3 to 7 years. These warm El Niño events are superimposed on seasonal warming cycles. The salinity field shows similar variability due to the same sets of climatic, and seasonal mechanisms. El Niño events bring floods causing river discharges of fresh water which depress the salinities of the coastal oceans in the vicinities of river mouths. Similar variations occur inter-annually as seasonal changes in wind patterns move different water masses with different salinities into and out of the

Southern California Bight. Therefore, the local environment already has a natural degree of variability in temperature and salinity on which the activities of the generating station and desalination plants are superimposed. In addition the ocean forcing functions that will mix and carry away the heat and concentrated seawater resulting from these two activities are likewise modulated by El Niño events, seasonal changes in weather patterns and by diurnal and semi-diurnal changes in tidal stage. Even the generating station's production is effected by climatic, seasonal, and daily changes in user demand, with corresponding adjustments in the volume of sea water consumed by the plant and the amount of waste heat introduced into the coastal waters. We will explore the potential effect on the discharge of concentrated sea water from the desalination plant associated with the interplay between the operational variability of the host generating station and the environmental variability of the receiving water by computing each possible outcome among the 7,523 separate combinations of potential inputs contained Figures 3.23 and 3.24.

The historic boundary conditions from Figure 3.23 and the forcing functions from Figure 3.24 were sequentially input into the model, producing daily solutions for the salinity field discharged from the AES Huntington Beach outfall due to the combined operations of the generating station and the desalination plant. The input stream of seven controlling variables from Figures 3.23 & 3.24 produced 7,523 daily solutions for the salinity field around the outfall. A numerical scan of each of these daily solutions searched for the maximum salinity at distances of 0, 50, 100, 150, 300, 500, 1,000 and 2,000 meters away from the outfall in all directions. These increments of search radii were selected to resolve both the high saline core of the discharge plume as well as the extent of the associated broad-scale salt wedge

feature having weakly elevated salinities. The solution scans searched for salinity maximums in both the water column and along the seafloor. For each search radius, the largest salinity found in any direction away from the outfall was entered into a histogram bin for ultimately assembling a probability density function and cumulative probability from the 7,523 outcomes. Histogram bins were constructed at salinity increments of 0.4 ppt. The bins were then summed to calculate the cumulative probability distribution. The histogram recurrence analysis was repeated for both warm water discharges at a Delta-T of $\Delta T = 18$ °F (10 °C) and a cold water discharge at a Delta-T of 0 °.

When reading the histogram plots in this section (Figures 5.2 - 5.15 and 5.21 - 5.34) , the following conventions are used:

1) In the water column, vertical red bars are the histogram bins for a discharge Delta-T of $\Delta T = 18$ °F (10 °C), while the vertical blue bars are the histogram bins of cold water discharge at $\Delta T = 0$ °C.

2) On the sea floor, vertical green bars are the histogram bins for a discharge Delta-T of $\Delta T = 18$ °F (10 °C), while the vertical blue bars are the histogram bins of cold water discharge at $\Delta T = 0$ °C.

3) For both water column and sea floor histograms, only those histogram bins for cold water outcomes ($\Delta T = 0$ °C) that exceed the salinity of the normal warm water discharges ($\Delta T = 10$ °C) are shown.

4) For both water column and sea floor plots, the calculation of the cumulative probability (blue line) is based on the highest salinity outcomes, regardless of whether they are due to warm or cold water discharges. Thus the cumulative probability distribution always includes ultimate worst case. For reference, the maximum salinity from the low flow case scenario from

Section 4 is shown as a dashed, black vertical line.

A) Saline Anomalies at the Outfall

Figure 5.1 gives the histogram and cumulative probability of daily maximum salinites at mid depth directly over the outfall (0 meters from outfall). These results are in the core of the discharge jet directed vertically upward toward the sea surface (see Figures 4.4, 4.5, 4.12 & 4.13). These salinities are nearly the same as end-of-pipe values other than for the mixing that occurred over the short distance between the top of the outfall and the middle of the water column. Hence the statistical character of these salinites are controlled by the interplay between historic plant flow rates and historic ocean salinities between 1980 and July 2000. Inspection of the post-1987 portion of the flow rate record in Figure 3.23a reveals that plant operations have been limited primarily to only two modes: either one generating unit operating at 126.7 mgd or 2 generating units at 253.4 mgd. Figure 5.1 shows that when the flow rate history in Figure 3.23a is applied to the ocean salinity variation in Figure 3.21 or 3.23b, the resulting end-of-pipe salinity variation from the combined discharge of the desalination plant and generating station will have a bi-modal probability density distribution. This bi-modal behavior is a direct consequence of the historic 2-mode production levels of the generating station. Although there were instances of the plant operating with three and four generating units in the first seven years of the 1980- July 2000 period of record (see Figure 3.22 and 3.23a) the preponderance of the record shows that the plant supplied only 2 different flow rates (127.6 or 253.4 mgd) most of the time. In the long term desalination simulations based on this historic operating record, this

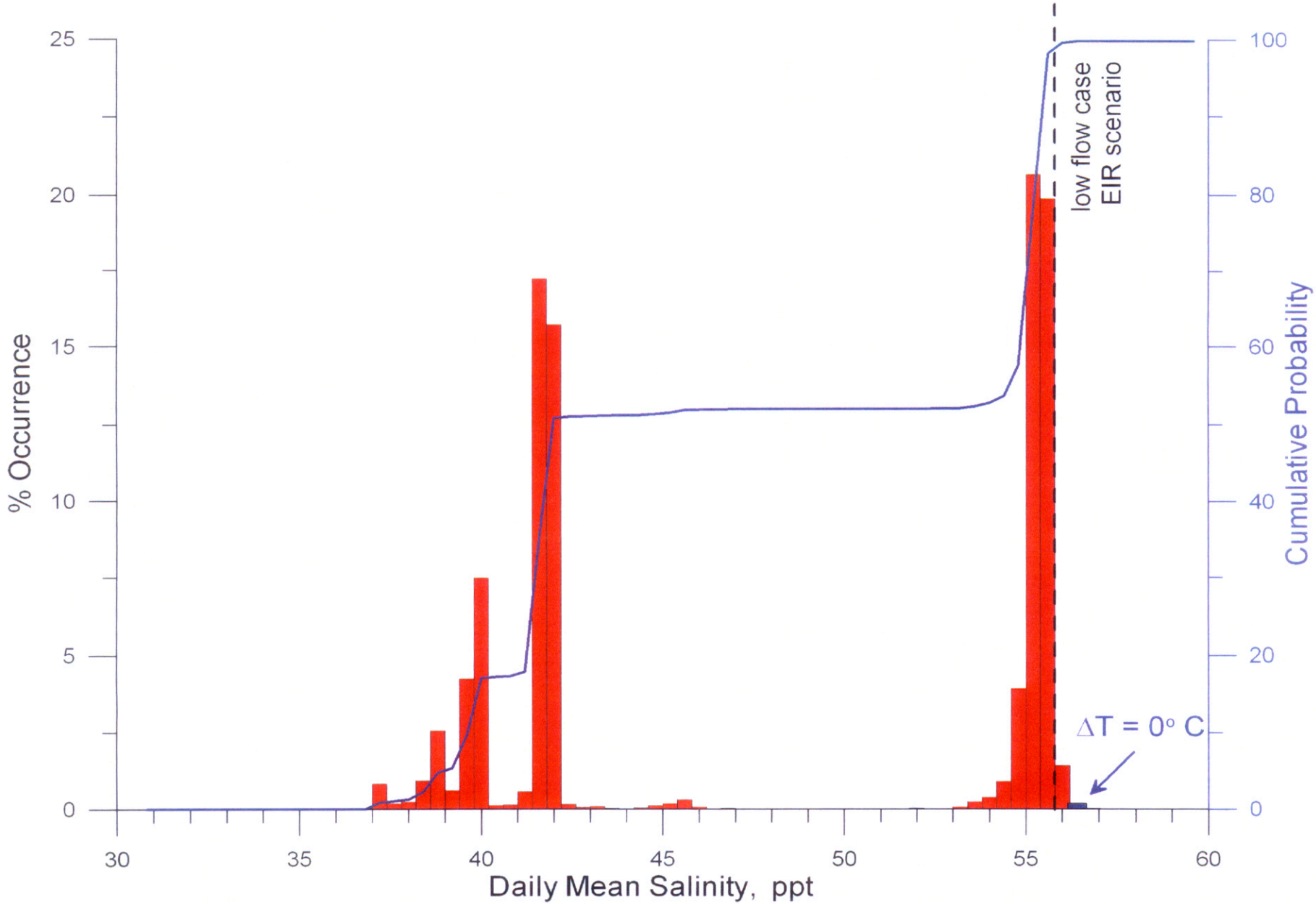

Figure 5.1. Histogram of daily maximum salinity at mid-depth and 0 meters from the AES outfall for desalination production rate of 50 mgd. Percent occurrence based on historic observations of ocean mixing and water mass mass properties, and AES daily plant flow rates, 1980-2000.

gives only 2 different flow rates for diluting the 50 mgd stream of concentrated sea salts from the desalination plant. Consequently there are only two preponderant discharge salinities, because the natural variability in ocean salinity (10%) is small compared to 100% variability (127.6 vs 253.4 mgd) in plant flow rate.

Figure 5.1 also shows that the combined end-of-pipe salinity will vary from a minimum of 37 ppt to a maximum of 56.4 ppt for cold water discharges ($\Delta T = 0$ °C) . The two predominantly recurring peaks in the probability density function for end-of -pipe salinity are centered at 41.6 ppt and 55.2 ppt, consistent with the average and low flow case values , respectively, as assigned to end-of-pipe sea salt concentrations (see Table 6, Section 3). The median (50% cumulative probability) salinity is actually 42.0 ppt. The maximum salinity of the warm water discharge ($\Delta T = 10$ °C) is 55.4 ppt, also in line with the low flow case scenario presented in the EIR. However the cumulative probability of the Section 4 low flow case salinity turns out to be only 82% . The discrepancy is due to the low flow rate bias in the flow rate statistics during the plant re-fitting of the 1990's . The absence of thermal agitation in the cold water discharge results in an increase of one part per thousand (1 ppt) in the salinity at mid depth of the water column directly over the outfall. The cold water exceedence of 1 ppt occurs about 20% of the time throughout the 20.5-year period of record. However, we will show in the subsequent sections that this initially higher water column salinity at the outfall is quickly suppressed with increasing depth or distance away from the outfall. This occurs because the cold water discharge is heavier in the absence of thermal expansion from the waste heat. The heavier discharge subsides more rapidly from its initial upward trajectory after leaving the outfall chimney. The subsidence is itself a mixing mechanism, engaging the full water column in the dilution volume. The more rapid the subsidence, the

more vigorous the vertical stirring of that dilution volume becomes.

Figure 5.2 gives the histogram and cumulative probability of daily maximum salinites on the sea floor at the base of the outfall (0 meters from outfall). The median (50% cumulative probability) salinity is 38.8 ppt, about 1.2 ppt higher than with the average case scenario presented in Section 4; but the maximum warm water discharge salinity is 48.2 ppt, on par with the low flow case scenario in Section 4. The cold water discharge salinities exceed the Section low flow case scenario by 0.3 ppt but, are a less than 1% occurrence events for which the cumulative probability greater than 99%.

While the water column and sea floor salinities above and at the foot of the outfall appear to be in-line with the average and low flow case results in Section 4, the frequency of occurrence of the low flow case extremum are not negligible. In the water column above the outfall, 55 ppt is found about 22 % of the time from the 1980- July 2000 records, and all the outcomes in the high flow rate peak of the probability density distribution around 55ppt account for 48% of the outcomes. While 48.3 ppt is found on the seafloor less than 1 % of the time, 47.6 ppt would occur about 28 % of the time, and all of the collection of sea floor realizations in the low flow rate peak centered at 47.5 ppt account for 48% of the outcomes; but again, based on the historic plant operating patterns during the 1980- July 2000 time frame. However, at the outfall salinity is controlled by in-the -pipe conditions rather than by ambient mixing or advection by ocean processes. Because the plant operated very close to the low flow case scenario flow rate throughout the 1990's (see Figure 3.22), the salinity extremes at the outfall in both the water column and

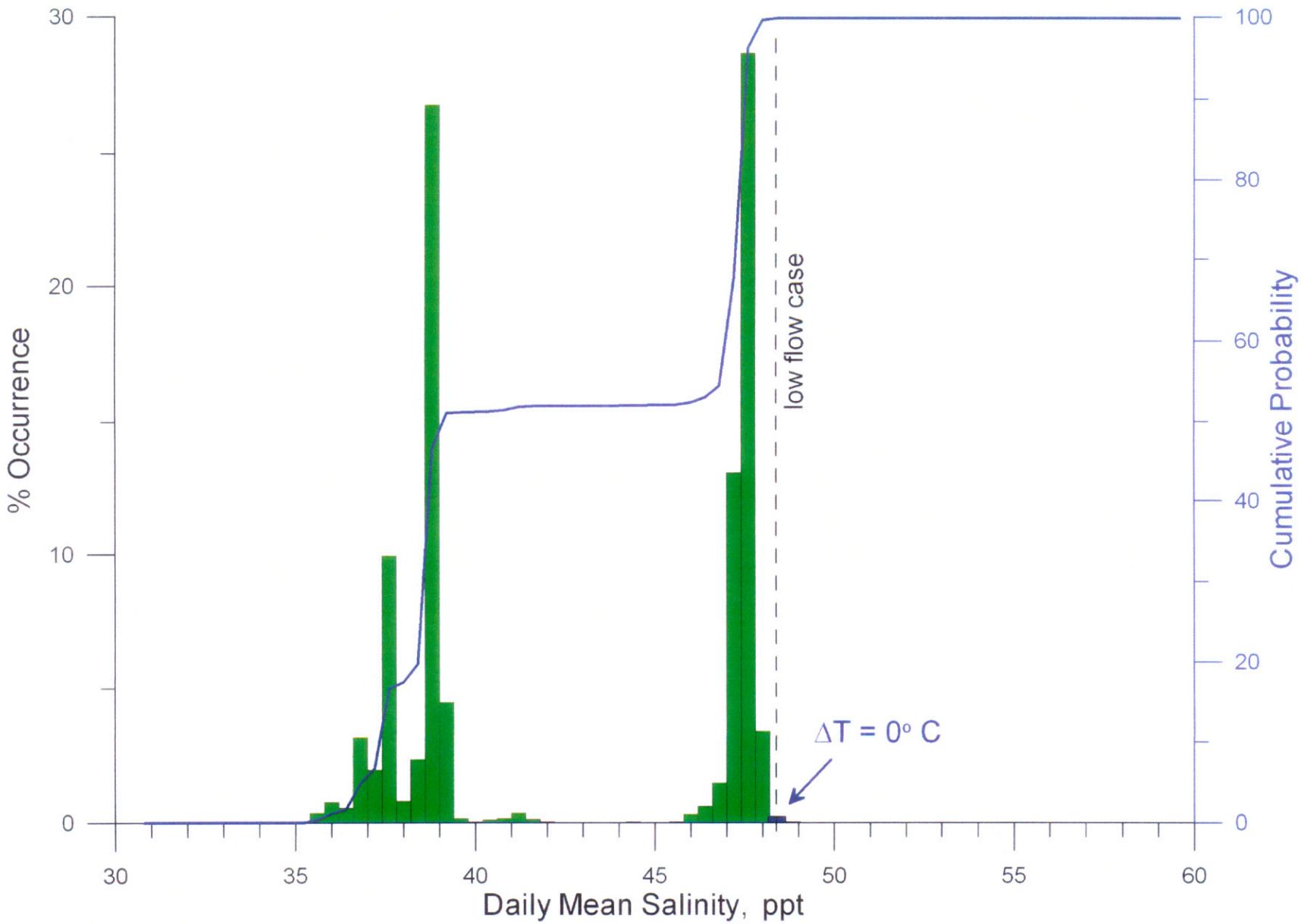

Figure 5.2. Histogram of daily maximum salinity at the bottom and 0 meters from the AES outfall for desalination production rate of 50 mgd. Percent occurrence based on historic observations of ocean mixing and water mass mass properties, and AES daily plant flow rates, 1980-2000.

on the sea floor are also at or near low flow case values a disproportionately high percentage of the time. We will find in subsequent sections that as we get further away from the outfall, the occurrence statistics of the ocean processes will begin dominate the recurrence behavior of the salinity extremes.

B) Saline Anomalies 50 meters from the Outfall

Figure 5.3 shows that a substantial amount of dilution of the salinity maximums and means occurs in the water column over the first 50 meters away from the outfall due to the mixing occurring in the inner core of the discharge plume. The dynamical effect of this mixing shifts the two primary peaks of the probability density to lower salinity values and to broaden those peaks over a wider salinity range. Mixing reduces the median salinity to 38.2 ppt and the maximum salinity to 47 ppt, both consistent with the results presented in Section 4 for average and low flow case. There were no cold water outcomes ($\Delta T = 0$ °C) that exceeded the Section 4 low flow case scenario. The probability density distribution 50 meters from the outfall remains bi-modal with a low flow rate peak centered on 45.4 ppt that accounts for 48% of the outcomes and a mid-flow rate peak centered at 37.4 ppt accounting for 52 % of the outcomes. The low flow rate peak is associated with only one operational generating unit while the mid-flow rate peak is due to two generating units on line.

In Figure 5.4 we find similar bi-model histograms of probability density and cumulative probability on the sea floor 50 meters away from the outfall. The salinity peaks and maximums are less due to the additional dilution that occurs as the plume sinks from mid-depth to the bottom. For warm water discharges, the

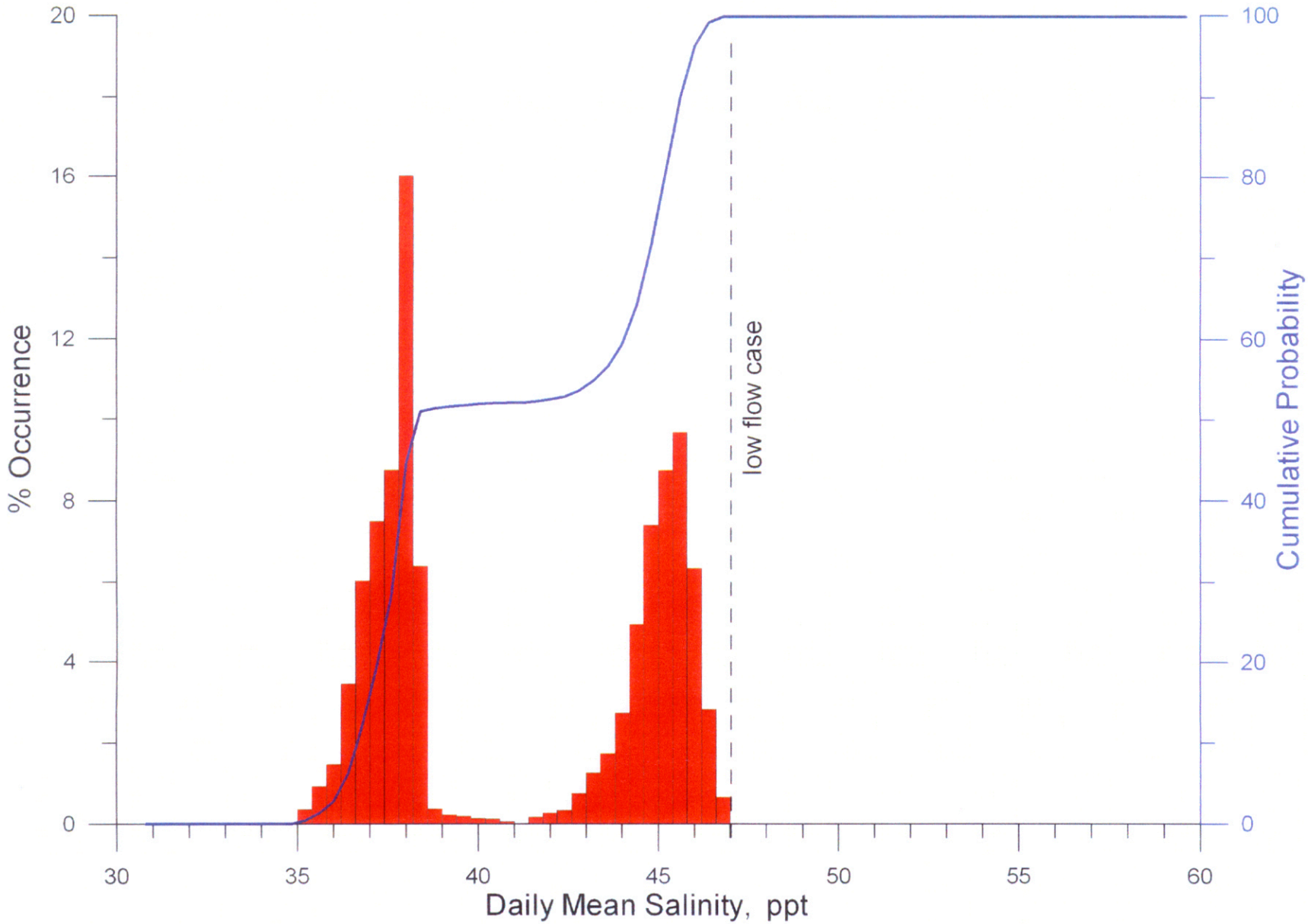

Figure 5.3. Histogram of daily maximum salinity at mid-depth and 50 meters from the AES outfall for desalination production rate of 50 mgd. Percent occurrence based on historic observations of ocean mixing and water mass mass properties, and AES daily plant flow rates, 1980-2000.

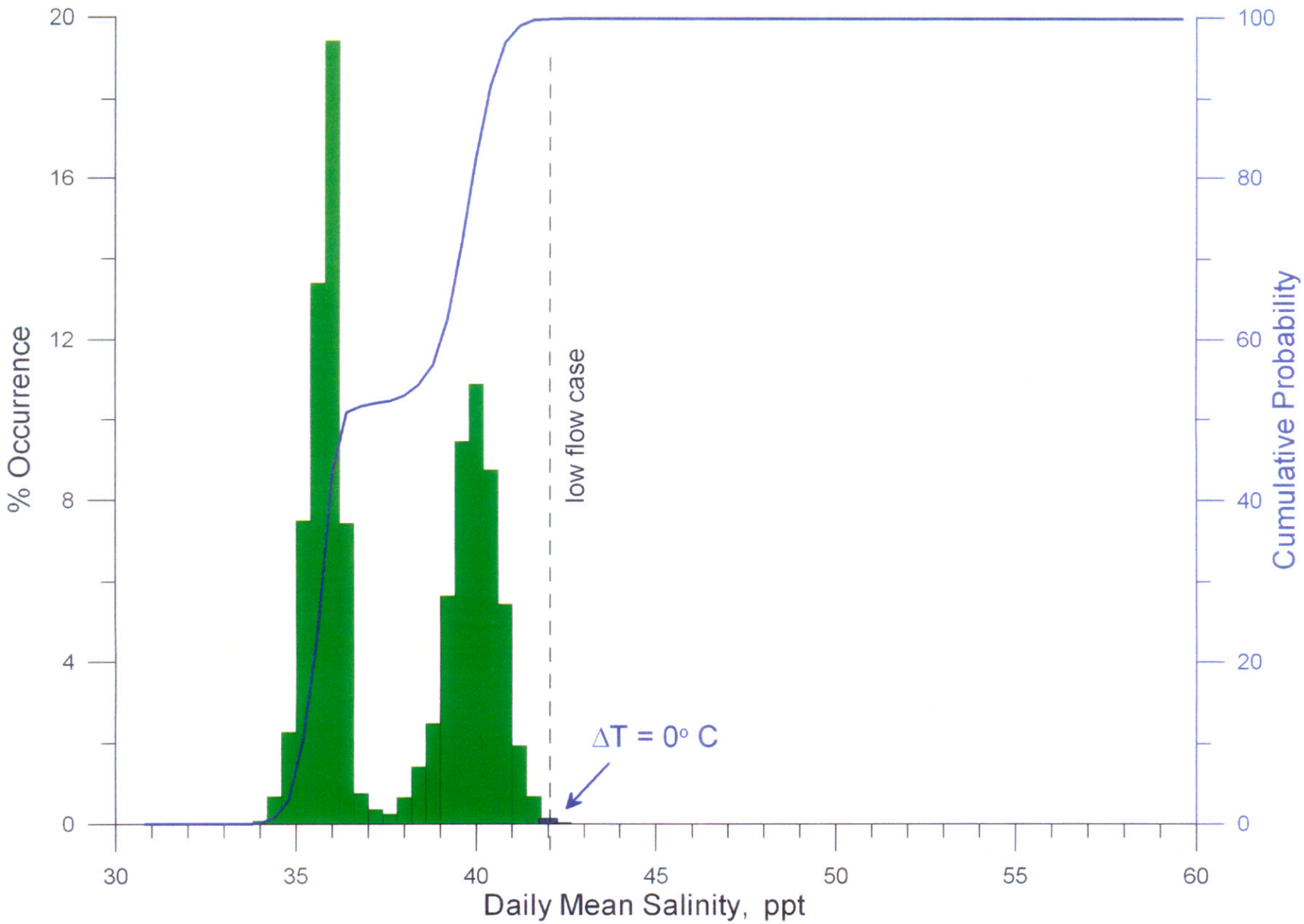

Figure 5.4. Histogram of daily maximum salinity at the bottom and 50 meters from the AES outfall for desalination production rate of 50 mgd. Percent occurrence based on historic observations of ocean mixing and water mass mass properties, and AES daily plant flow rates, 1980-2000.

salinity maximum is 41.8 ppt, while the cold water discharge reaches 42 ppt, both in line with the Section 4 low flow case scenario. The median salinity here on the outer edge of the inner core is 36.2 ppt, also comparable to the Section 4 average case scenario. The low flow rate recurrence peak in the sea floor probability density function is centered at 40 ppt and accounts for about 48% of the outcomes in the 1980-July 2002 record. The mid-flow rate recurrence peak is centered at 36 ppt and accounts for about 52% of the outcomes.

C) Saline Anomalies 100 meters from the Outfall

Here we enter the outer core of the discharge plume where advective entrainment of surrounding water by the residual upward momentum of the discharge jet causes further dilution (see Figures 4.4, 4.5, 4.12 & 4.13). As a result, further shifts towards lower salinities occur in both the low and mid-flow rate peaks of the water column probability density function (histogram) in Figure 5.5. The low flow rate peak is broader and is centered at about 43 ppt, accounting for about 47 % of the outcomes. Maximum salinity in the water column 100 meters from the outfall is 46 ppt, consistent with the Section 4 low flow case scenario and independent of warm vs cold water discharges. The mid- flow rate peak is shifted down to 36.6 ppt and accounts for 53% of the outcomes. The median water column salinity is 37 ppt. Comparing Figures 5.5 and 5.3 indicates that the advective entrainment effects in the inner portion of the outer core are not especially vigorous, reducing salinity maximums and means by about 1ppt, but significantly broadening the low and high flow rate peaks and thereby reducing the degree of sorting between them.

Figure 5.6 gives the histogram (probability density) and cumulative

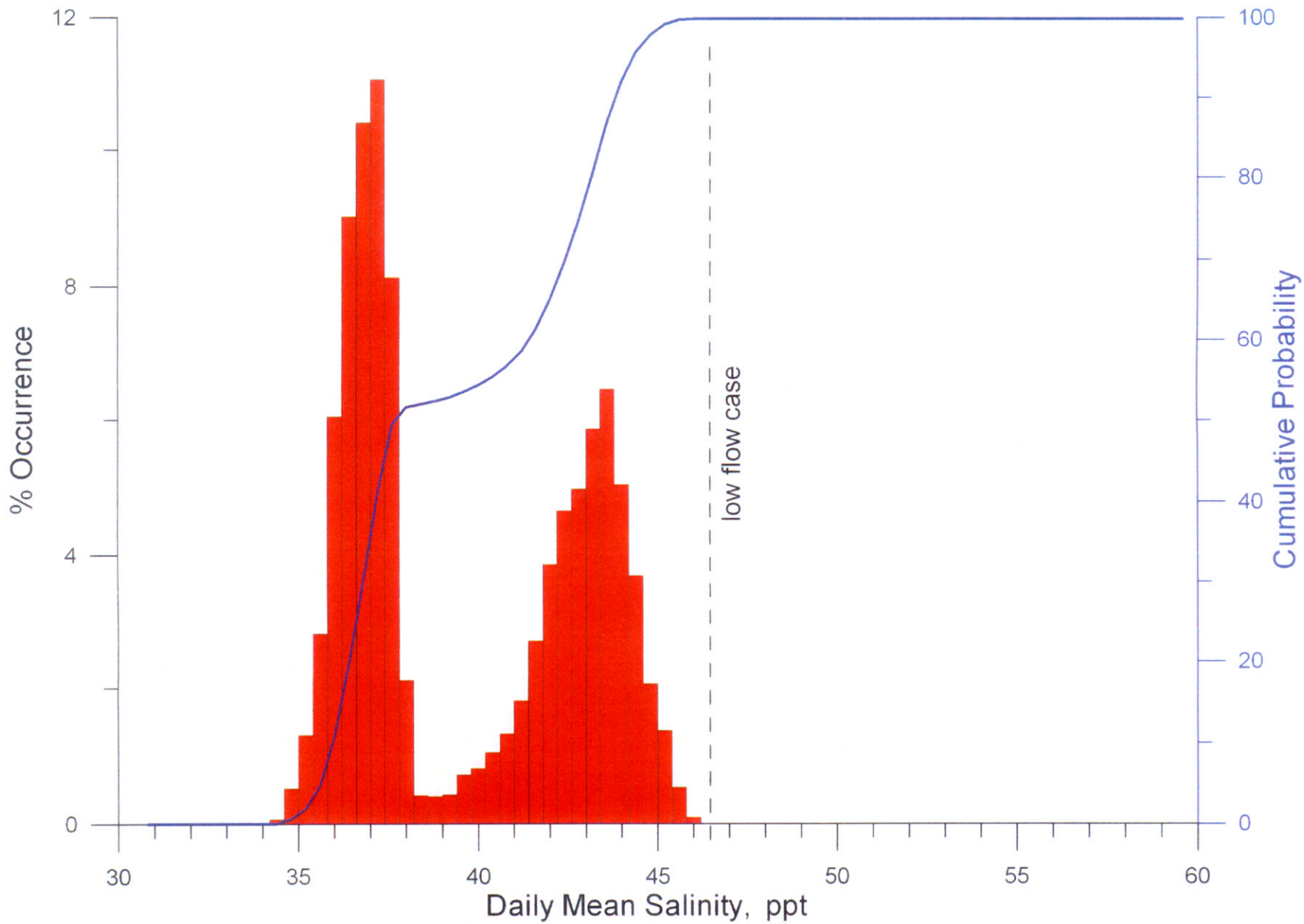

Figure 5.5. Histogram of daily maximum salinity at mid-depth and 100 meters from the AES outfall for desalination production rate of 50 mgd. Percent occurrence based on historic observations of ocean mixing and water mass mass properties, and AES daily plant flow rates, 1980-2000.

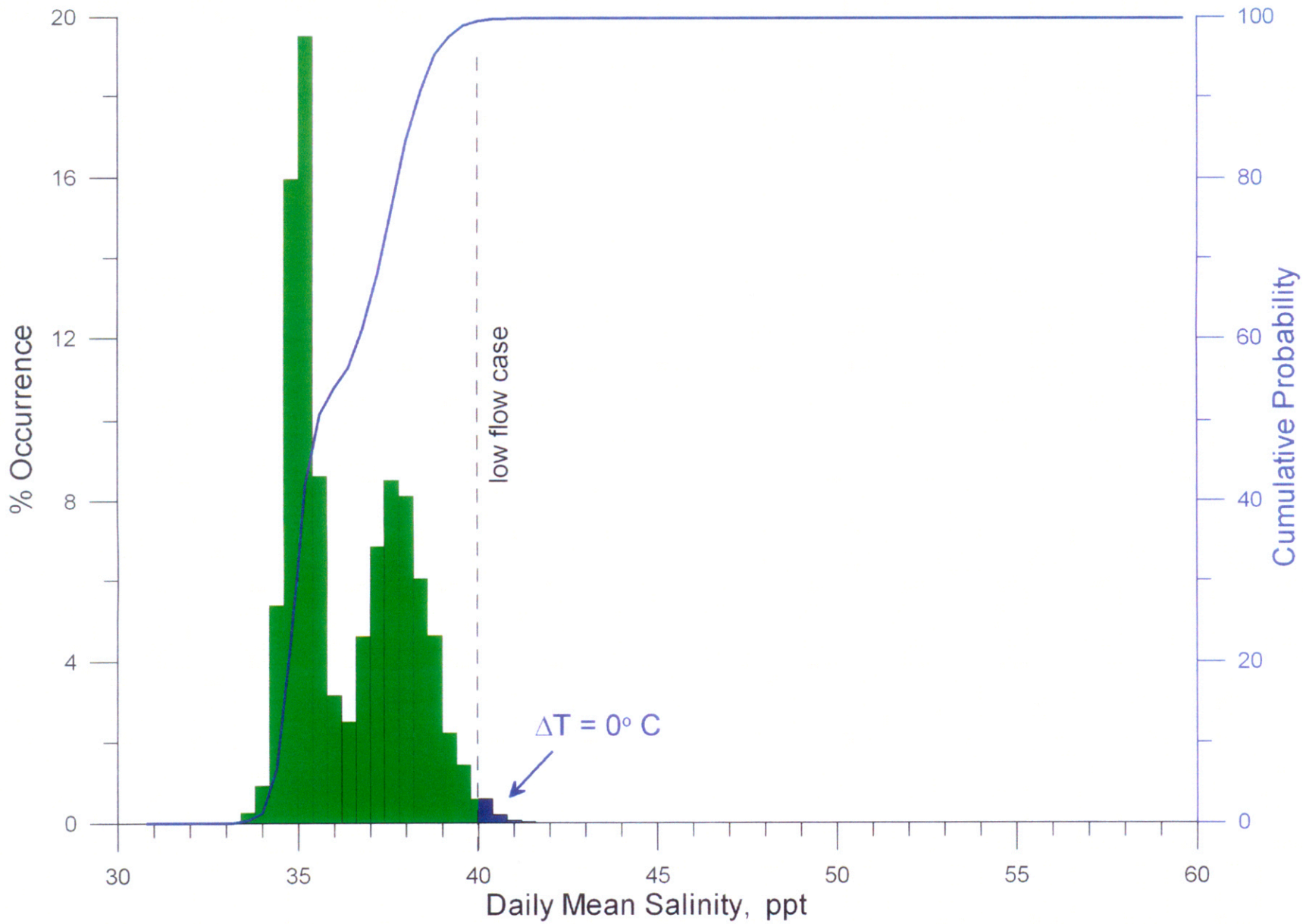

Figure 5.6. Histogram of daily maximum salinity at the bottom and 100 meters from the AES outfall for desalination production rate of 50 mgd. Percent occurrence based on historic observations of ocean mixing and water mass mass properties, and AES daily plant flow rates, 1980-2000.

probability of daily maximum salinites on the sea floor at 100 meters away from the base of the outfall. Here the median sea floor salinity is 35.5 ppt, and the maximum warm water discharge salinity is 40 ppt both consistent with the average and low flow case scenarios presented in Section 4. However the, the heavier cold water discharge produces salinity extremses reaching 41.3 ppt about 3% of the time during the 1980- July 2000 record. The low- flow rate peak centered on 37.8 ppt accounts for 43% of the outcomes, while the mid-flow rate peak centered on 35 ppt accounts for 57%. In both Figures 5.4 and 5.5 it is noted that the low flow rate peak is broader. This is due to the higher salinity of the low flow rate peak which results in larger concentration gradients relative to the surrounding ambient water mass, thereby yielding larger diffusive fluxes than for the mid-flow rate peak.

D) Saline Anomalies 150 meters from the Outfall

At this distance from the outfall we are in about the middle of the outer core in the down drift direction and at the outer edge in the cross shore direction (see Figures 4.4, 4.5, 4.12 & 4.13). The reason for this directional asymmetry is the along shore stretching of the plume by the ebb-dominated tidal currents that have a net drift downcoast towards the Santa Ana River over any given 24 hour period (see Figures 4.1 - 4.3 and 4.10 - 4.12).

Figure 5.7 gives the histogram (probability density function) and cumulative probability of daily maximum salinites at mid depth in the water column at a distance of 150 meters from the outfall. The continued broadening of the low flow rate peak of the probability density function is becoming more apparent at increasingly larger distances away from the outfall. In fact the low-flow and mid-

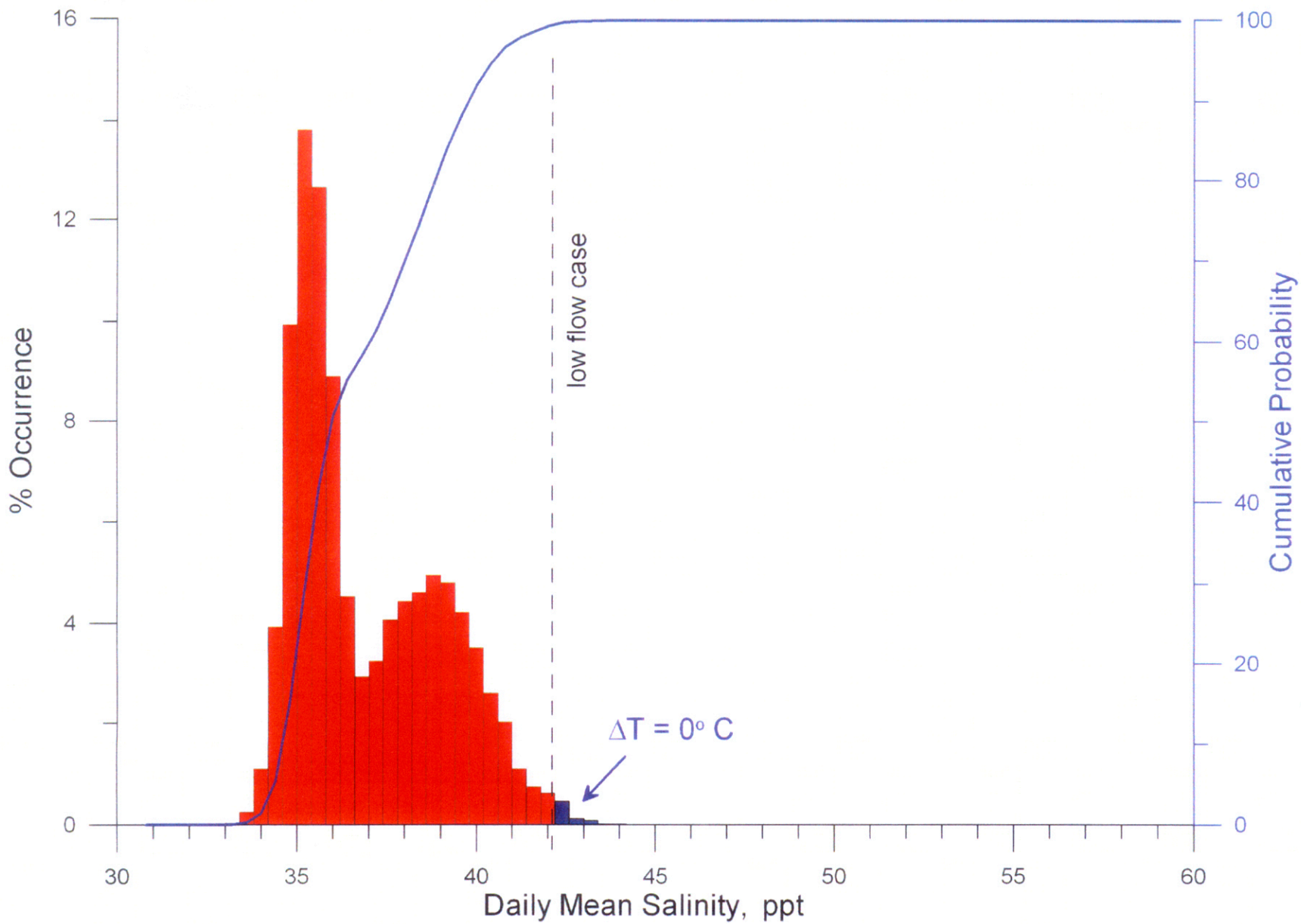

Figure 5.7. Histogram of daily maximum salinity at mid-depth and 150 meters from the AES outfall for desalination production rate of 50 mgd. Percent occurrence based on historic observations of ocean mixing and water mass mass properties, and AES daily plant flow rates, 1980-2000.

flow rate peaks of the probability density function are beginning to merge. The low flow rate peak is centered on 39 ppt and accounts for 42% of the outcomes, but extends to maximum warm water discharge salinities as high as 42.2 ppt. The highest warm water salinity matches the Section 4 low flow case scenario, but cold water discharges reach an ultimate maximium salinity of 43.4 ppt and account for about 3% of the outcomes. The median water column salinity (50% cumulative probability) is 36 ppt. The mid-flow rate peak in the probability density distribution is centered on 35.2 ppt and makes up 58% of the total realizations.

Figure 5.8 gives the histogram (probability density) and cumulative probability of daily maximum salinites on the sea floor at 100 meters away from the base of the outfall. The median sea floor salinity is 35.0 ppt, and the highest warm water discharge salinity is 39 ppt, again both consistent with the average and low flow case scenarios presented in Section 4. The cold water discharge that results in greater density stratification produces highest salinities of 39.8 ppt that occur about 3 % of the time during the 1980- July 2000 record. The low- flow rate peak in the probability density distribution is centered on 37.0 ppt accounts for 42% of the outcomes, while the mid-flow rate peak centered on 34.8 ppt accounts for 58% of the modeled realizations. Comparing Figure 5.8 against Figure 5.7 it is interesting to note that the density stratification within the saline plume at a distance of 150 meters from the outfall is unstable, with higher salinities in the water column than on the sea floor. This indicates that subsidence is underway in the middle of the outer core, and that the mid-depth portion of the plume is in a state of overturning, thereby promoting vertical stirring and mixing. This effect is greatest for the low-flow rate portion of the probability distribution for which salinities are highest and the subsidence rates are greatest.

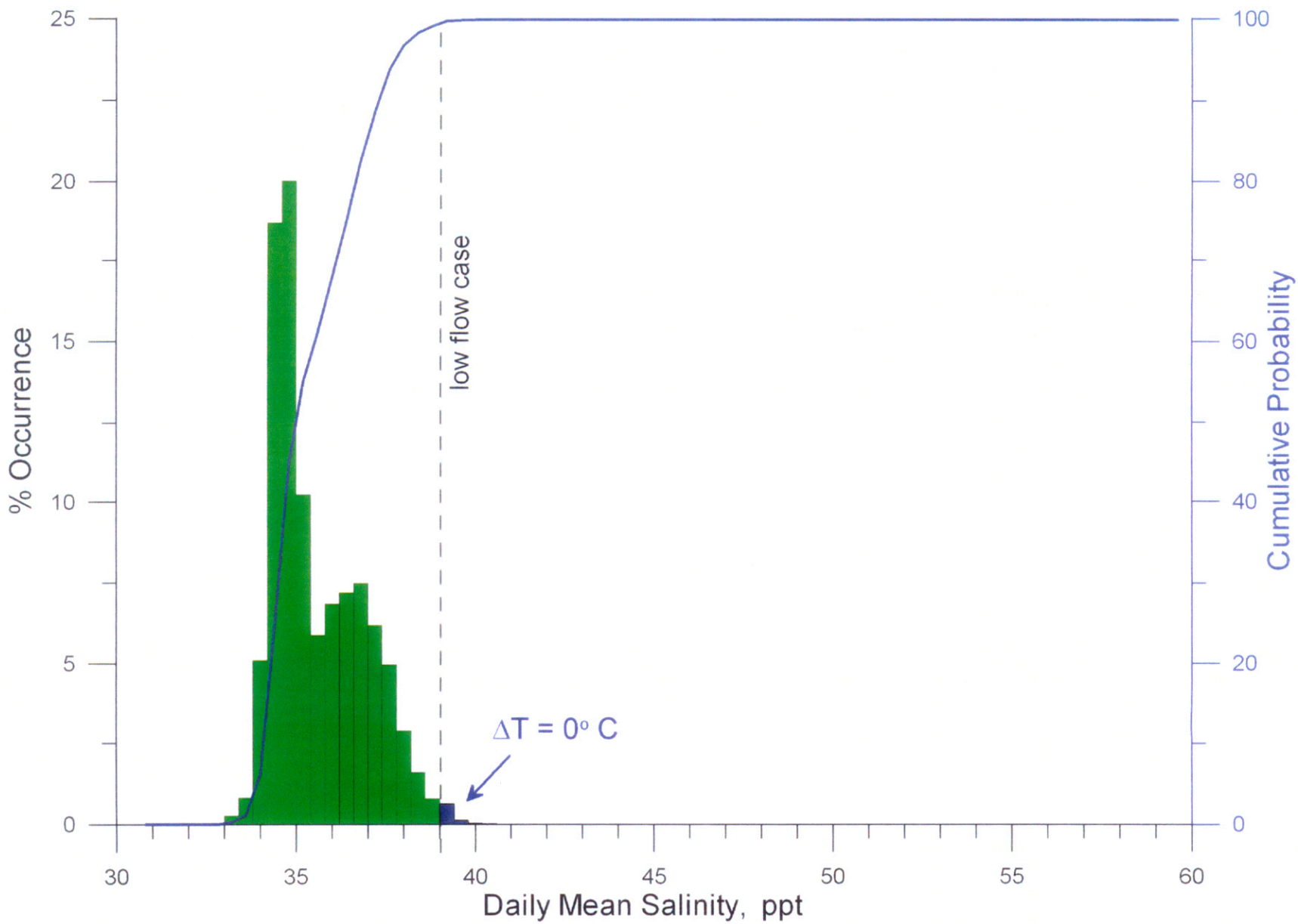

Figure 5.8. Histogram of daily maximum salinity at the bottom and 150 meters from the AES outfall for desalination production rate of 50 mgd. Percent occurrence based on historic observations of ocean mixing and water mass mass properties, and AES daily plant flow rates, 1980-2000.

E) Saline Anomalies 300 meters from the Outfall

At this distance from the out fall we are now at the outer edge of the outer core of the plume. The subsidence effects from the inverted salinity distribution in the outer core have now accelerated the mixing, particularly of the heavier low-flow rate salinity peak where salinities are highest, and have nearly homogenized the vertical salinity contrasts of the plume. Inspection of the probability density functions (histograms) of both the daily maximum salinites in the water column (Figure 5.9) and on the sea floor (Figure 5.10) show that low-flow rate peak has merged with the mid-flow rate peak, forming an asymmetric uni-model distribution with a shoulder on the on the high-salinity side of the distribution. Furthermore, both water column and sea floor distribution are very similar with only minor differences on a bin-by-bin comparison, indicating that the inverted salinity distribution that was characteristic of the plume closer to the outfall has been smeared nearly uniformly by mixing and subsidence. Since the bi-modal character of the histogram has been lost, we shall refer to its characteristics from here on as the *mid-flow rate peak and the low-flow rate shoulder*.

For the water column at 300 meters from the outfall (Figure 5.9) the median salinity is 34.6 ppt while the highest salinity for warm water discharges reaches 39 ppt, commensurate with the low flow case scenario results in Section 4. Cold water discharges increase the extreme water column salinity to 40.2 ppt. These cold water exceedence outcomes account for only 2% of the 7,523 number of realizations. The mid-flow rate peak of the distribution appears to be centered on 34.6 ppt and account for about 60% of the outcomes. Half of the outcomes in the low-flow rate shoulder are found either side of 36.2 ppt and altogether account for

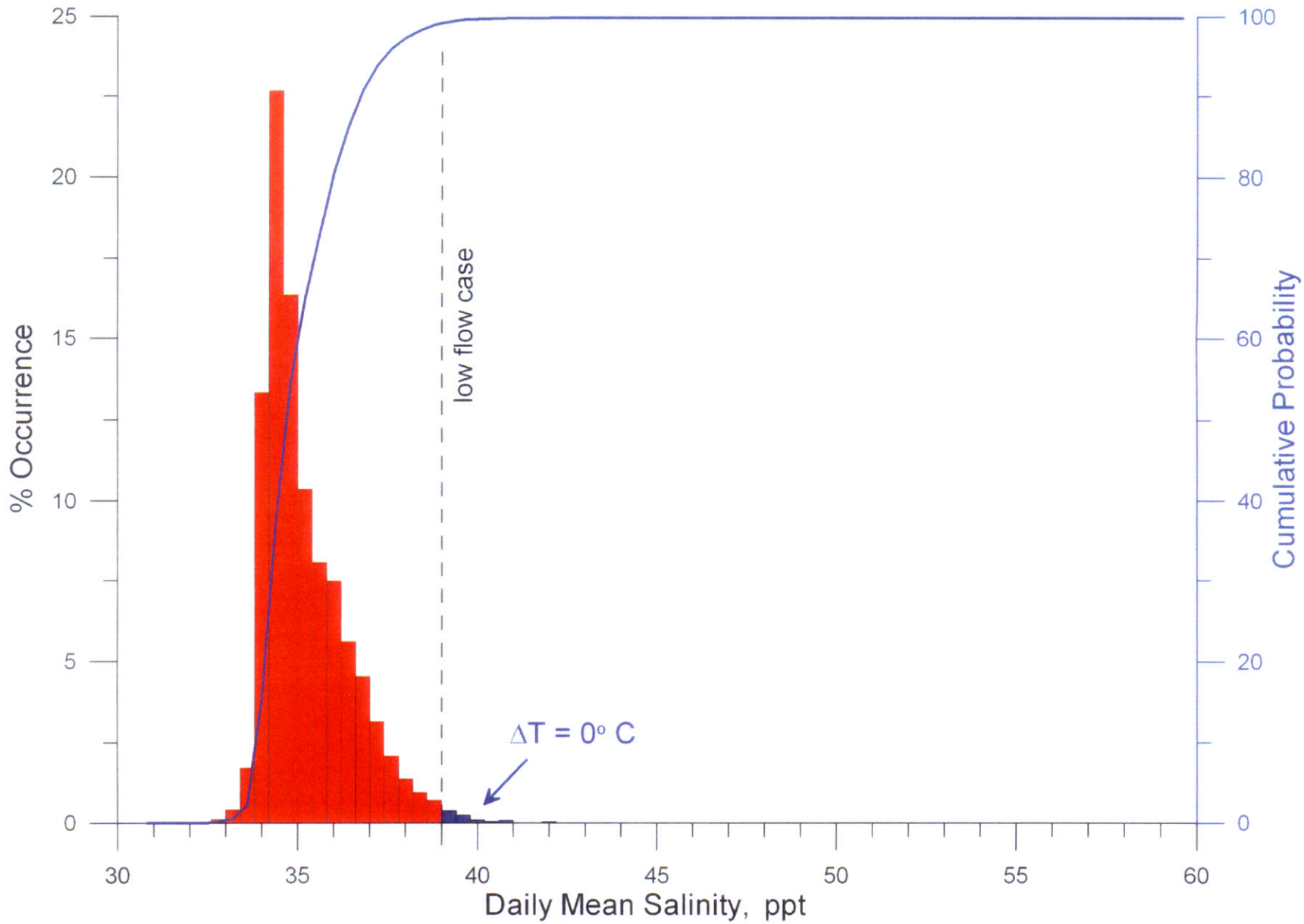

Figure 5.9. Histogram of daily maximum salinity at mid-depth and 300 meters from the AES outfall for desalination production rate of 50 mgd. Percent occurrence based on historic observations of ocean mixing and water mass mass properties, and AES daily plant flow rates, 1980-2000.

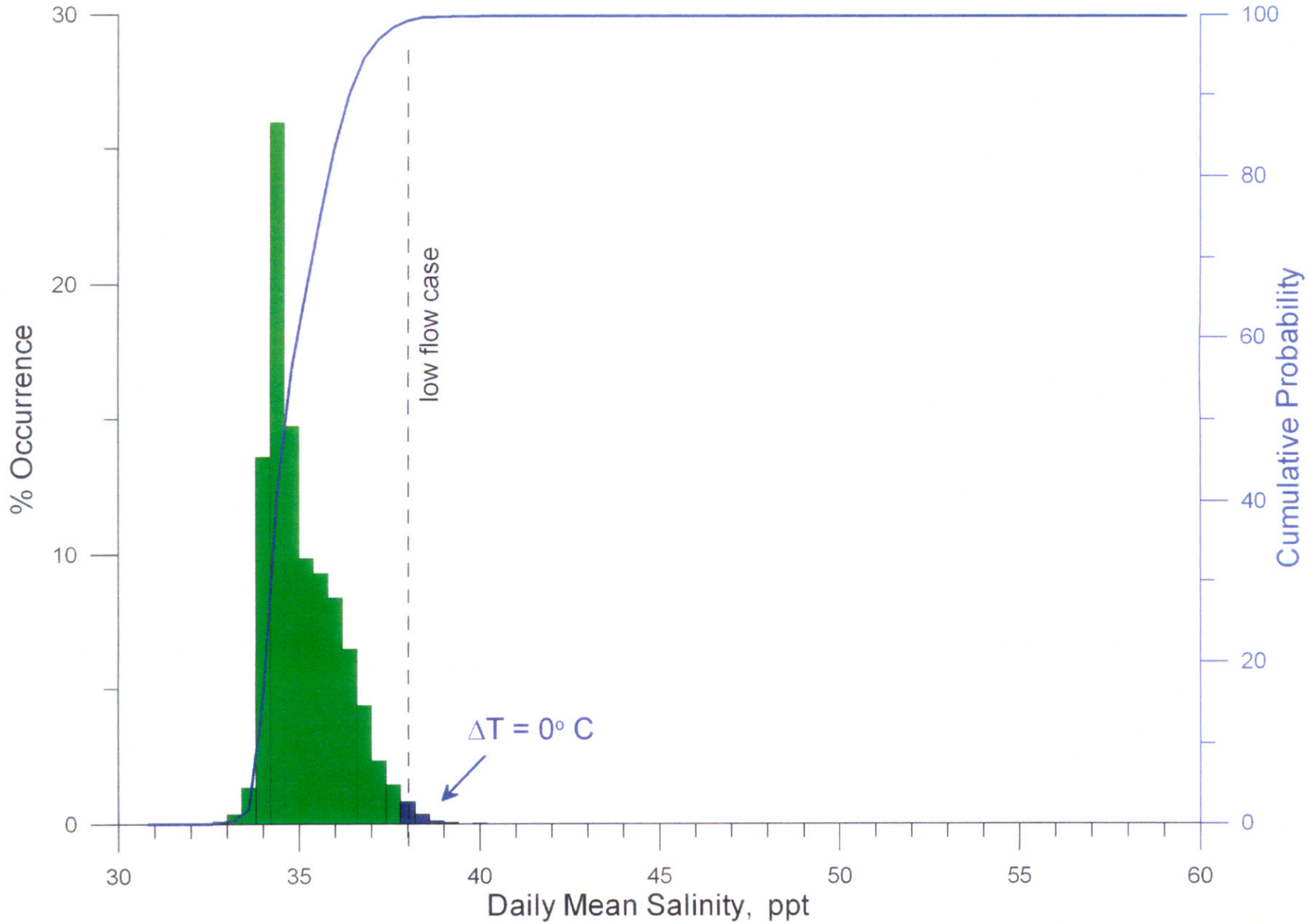

Figure 5.10. Histogram of daily maximum salinity at the bottom and 300 meters from the AES outfall for desalination production rate of 50 mgd. Percent occurrence based on historic observations of ocean mixing and water mass mass properties, and AES daily plant flow rates, 1980-2000.

40 % of the modeled realizations. For the sea floor salinities in Figure 5.10, the median salinity is also 34.6 ppt; the highest salinity for warm water discharges reaches 38.8 ppt; and cold water discharges reach a high of 40 ppt and exceed the warm water values about 3 % of the time. The mid-flow rate peak of the distribution also appears to be centered on 34.6 ppt accounting for about 60% of the outcomes. Half of the outcomes in the low-flow rate shoulder are found either side of 36.0 ppt and account for 40% of the realizations.

F) Saline Anomalies 500 meters from the Outfall

At 500 meters away from the outfall we are in the inner portions of the salt wedge region of the discharge plume. Here ambient ocean mixing by wind waves and currents takes over from discharge turbulence, entrainment and subsidence as the dominant dilution mechanisms. However, subsidence still continues throughout the salt wedge, but at slower rates as salinities come closer to ambient ocean water. The continuation of these subsidence effects causes the salt wedge to progressively become more stably stratified with increasing distance from the outfall. Comparison of the probability density functions (histograms) of the daily maximum salinites in the water column (Figure 5.11) versus those on the sea floor (Figure 5.12) show that the plume has become stably stratified on the low-flow rate shoulder of the distribution, with more outcomes of higher salinities occurring on the sea floor than in the water column. The other notable feature of these histograms, is that the uni-modal probability density distribution has become more narrow and shifted closer to the ambient ocean water distribution in Figure 3.21b. These traits become more pronounced at greater and greater distances from the outfall as will be shown in following sections. What they indicate is that

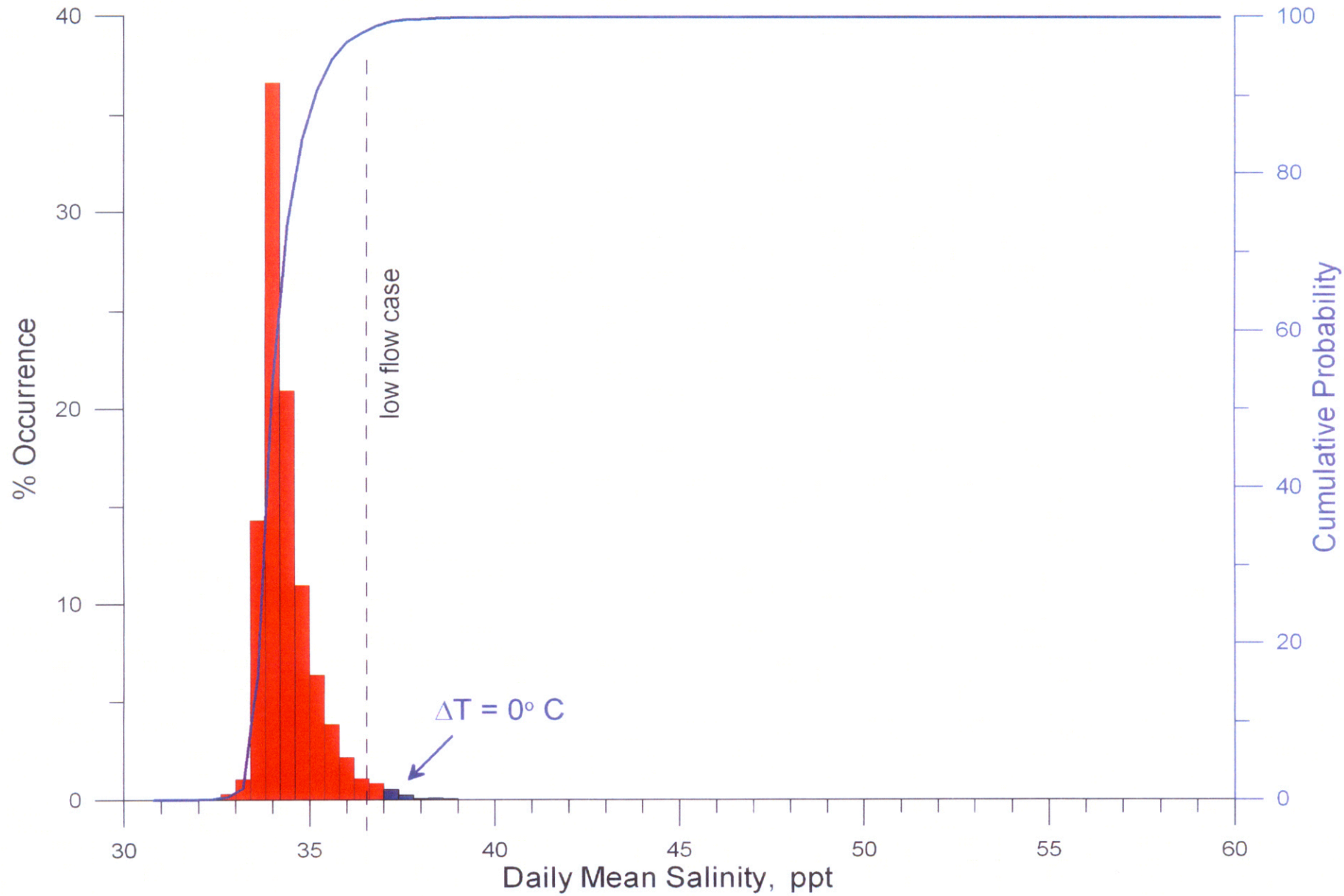

Figure 5.11. Histogram of daily maximum salinity at mid-depth and 500 meters from the AES outfall for desalination production rate of 50 mgd. Percent occurrence based on historic observations of ocean mixing and water mass mass properties, and AES daily plant flow rates, 1980-2000.

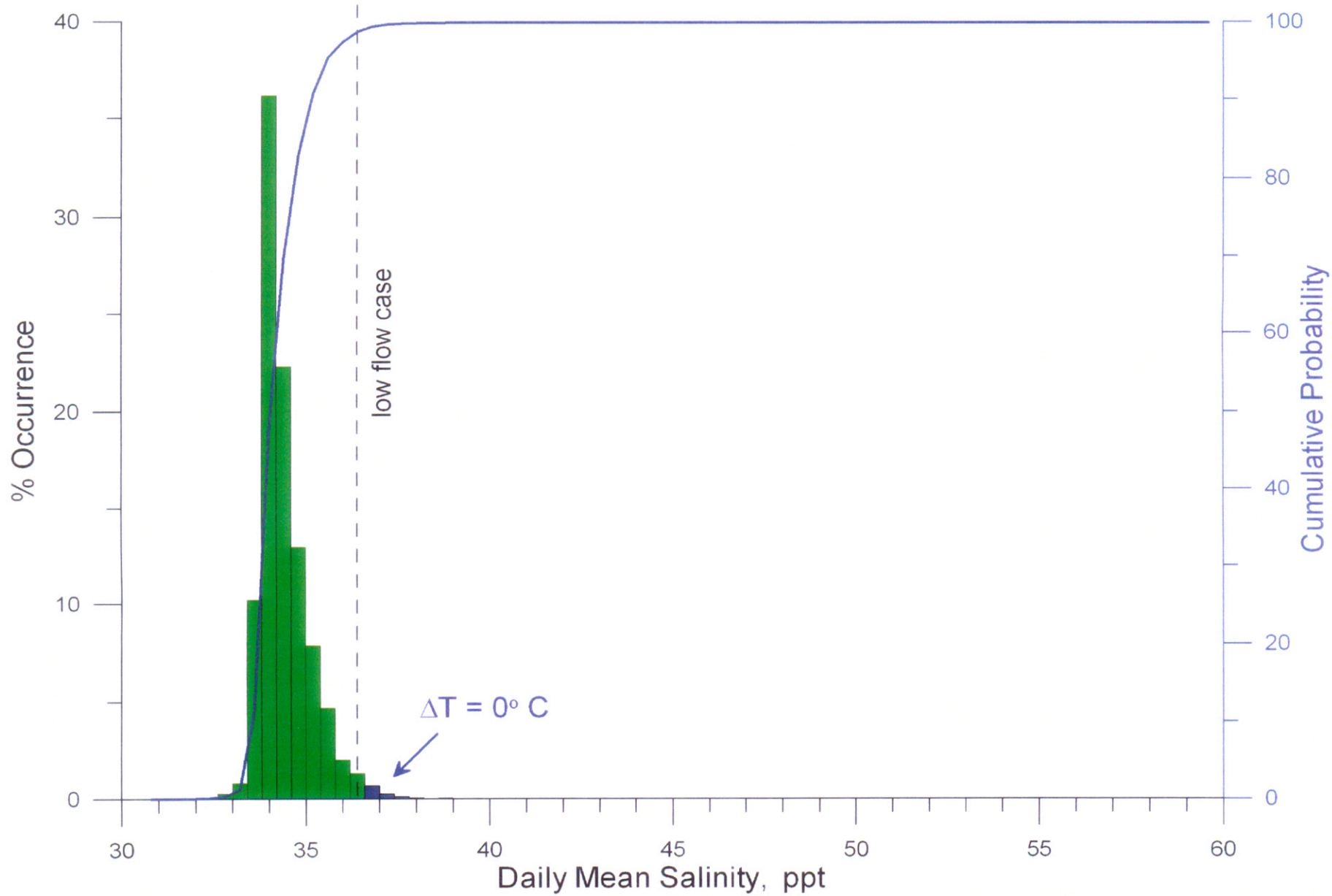

Figure 5.12. Histogram of daily maximum salinity at the bottom and 500 meters from the AES outfall for desalination production rate of 50 mgd. Percent occurrence based on historic observations of ocean mixing and water mass mass properties, and AES daily plant flow rates, 1980-2000.

differences in the salinity plume caused by different plant operating levels became less and less important in the salt wedge portion of the plume, as ambient ocean mixing dilutes the plume closer and closer to ambient ocean salinity.

At 500 meters from the outfall (Figure 11) the median water column salinity is 34.0 ppt while the highest salinity for warm water discharges reaches 36.6 ppt, consistent with results reported for the low flow case scenario results of Section 4. Cold water discharges increase the extreme water column salinity to 36.8 ppt. These cold water outcomes account for only 3% of the total number of realizations. The mid-flow rate peak of the distribution appears to be centered on 34.0 ppt and accounts for about 75% of the outcomes. Half of the outcomes in the low-flow rate shoulder are found either side of 35.0 ppt and altogether account for 25% of the modeled results. For the sea floor results in Figure 5.12, the median salinity is also 34.0 ppt; the highest salinity for warm water discharges reaches 36.2 ppt; and cold water discharges reach a high of 38.2 ppt. The number of cold water outcomes that exceed the highest warm water discharge occur about 4 % of the time. The mid-flow rate peak of the distribution also appears to be centered on 34.0 ppt accounting for about 70 % of the outcomes. Half of the outcomes in the low-flow rate shoulder are found either side of 35.2 ppt and account for 30% of the realizations.

G) Saline Anomalies 1000 meters from the Outfall

At 1,000 meters from the outfall, maximum daily salinities are always found in the long shore cross section of the salt wedge portion of the discharge plume (see Figure 4.13). Inspection of the probability density functions (histograms) of the daily maximum salinites in the water column (Figure 5.13) and on the sea floor

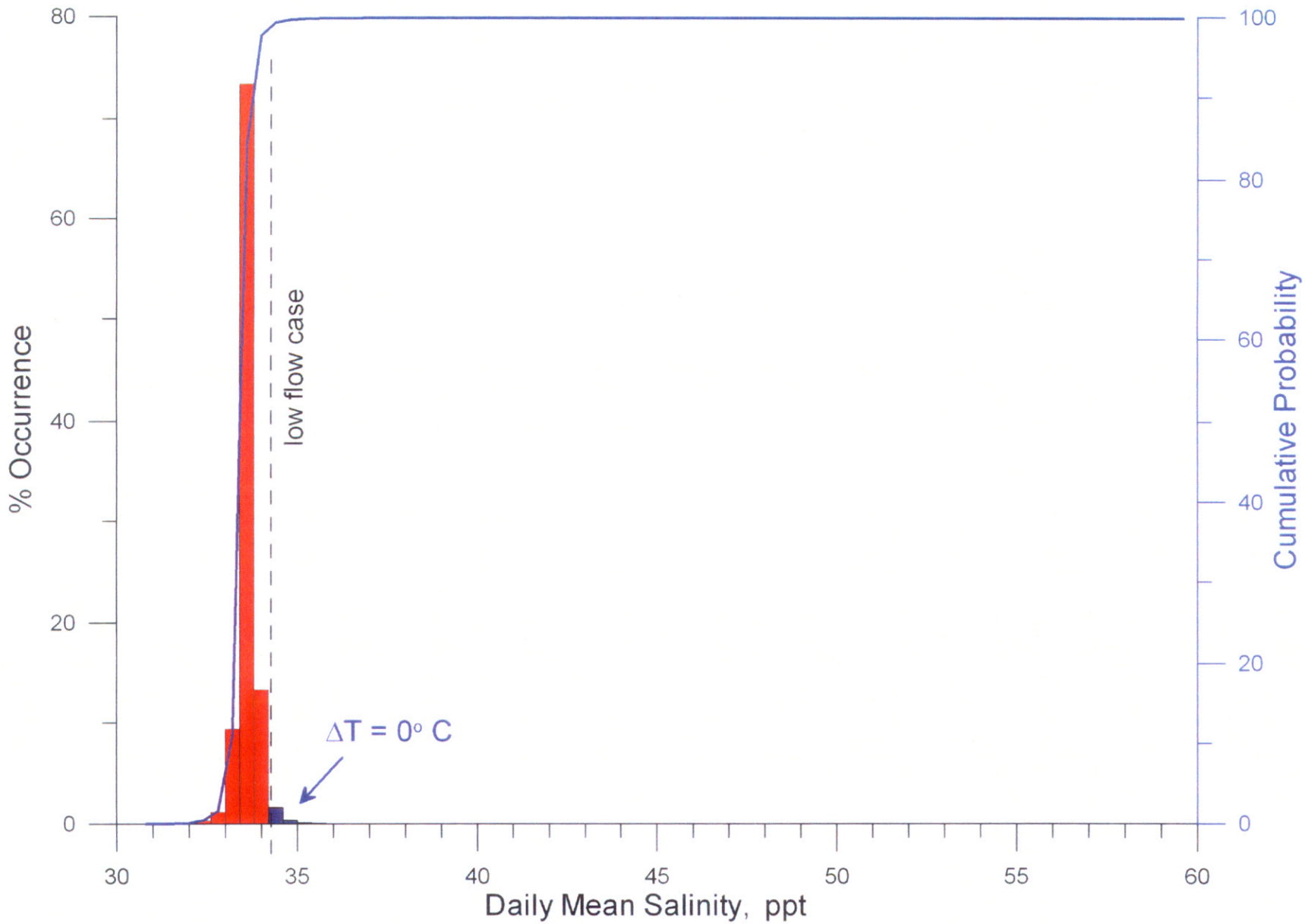

Figure 5.13. Histogram of daily maximum salinity at mid-depth and 1000 meters from the AES outfall for desalination production rate of 50 mgd. Percent occurrence based on historic observations of ocean mixing and water mass mass properties, and AES daily plant flow rates, 1980-2000.

(Figure 5.14) show that the uni-modal probability density distribution has become exceedingly narrow banded to the point that the low-flow rate shoulder is hardly recognizable. Both water column and sea floor distributions are very close to the ambient ocean water distribution in Figure 3.21b, indicating that dilution is nearly total (but not quite complete). In Figure 5.13, the median water column salinity is 33.6 ppt while the highest salinity for warm water discharges reaches 34.2 ppt, slightly less than results reported for the low flow case scenario results of Section 4. Cold water discharges increase the extreme water column salinity to 35.0 ppt. These cold water outcomes account for only 2% of the total number of realizations. The mid-flow rate peak of the distribution appears to be centered on 33.6 ppt and accounts for about 8% of the outcomes. Half of the outcomes in the low-flow rate shoulder are found either side of 34.0 ppt and altogether account for 18% of the model realizations. For the sea floor results in Figure 5.14, the median salinity is also 33.6 ppt; the highest salinity for warm water discharges reaches 34.6 ppt; and cold water discharges reach a high of 35.4 ppt. The number of cold water outcomes that exceed the highest warm water discharge occur about 1.5 % of the time. The mid-flow rate peak of the distribution also appears to be centered on 33.6 ppt accounting for about 82% of the outcomes. Half of the outcomes in the low-flow rate shoulder are found either side of 34.2 ppt and account for 18% of the realizations.

H) Saline Anomalies 2,000 meters from the Outfall

At 2,000 meters from the outfall, the discharge plume can be hardly distinguished from ambient ocean water, and dilution may be considered for all practical purposes, complete. Comparison of the probability density functions

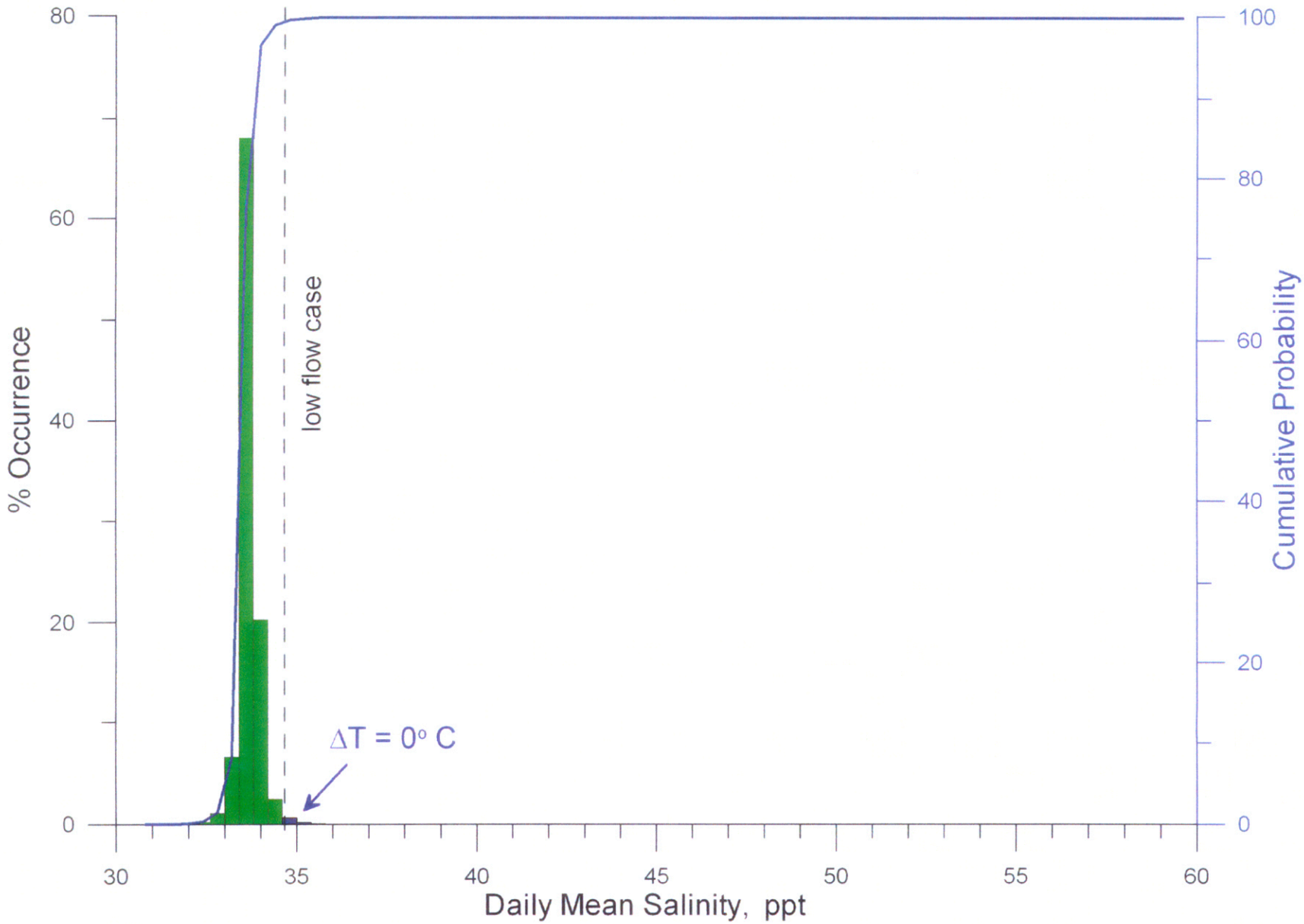

Figure 5.14. Histogram of daily maximum salinity at the bottom and 1000 meters from the AES outfall for desalination production rate of 50 mgd. Percent occurrence based on historic observations of ocean mixing and water mass mass properties, and AES daily plant flow rates, 1980-2000.

(histograms) of the daily maximum salinites in the water column (Figure 5.15) and on the sea floor (Figure 5.16) versus the ambient ocean water distribution in Figure 3.21b shows virtually no difference other than for a an enhancement of about 1.5% of the salinity bin centered on 34 ppt, largely the result of cold water discharge effects. Statistics for the water column and sea floor distributions are identical and essentially the same as ambient ocean water: median water column salinity is 33.5 ppt; maximum salinity is 34.3 ppt; minimum salinity is 31.1 ppt. The only change in the discharge plume 2,000 meters from the outfall is that salinities between 34.0 ppt and 34.3 ppt happen 2% of the time in the plume versus 0.3% of the time in ambient ocean water.

I) Summary of Long-Term Dilution Analysis:

An intensive set of hydrodynamic model runs produced 7,523 outcomes for the dispersion of the saline plume discharged from the AES Huntinton Beach outfall, as a result of piggy-backing a 50 mgd desalination plant on the back end of the generating station cooling loop. The modeled outcomes were the result of 20.5 year long continuous time series of daily records for seven controlling operational and environmental inputs. The period of record for these simultaneous sets of seven inputs was 1980 to July 2000. We were constrained to this particular historic period based on the availability of wave monitoring data. However, this period was probably atypical from the operational stand point because the generating station was under going re-fit and equipment modernization. These capital improvements limited plant production to either one or two generating units for much of the time, providing only 126.7 mgd or 253.4 mgd with which to

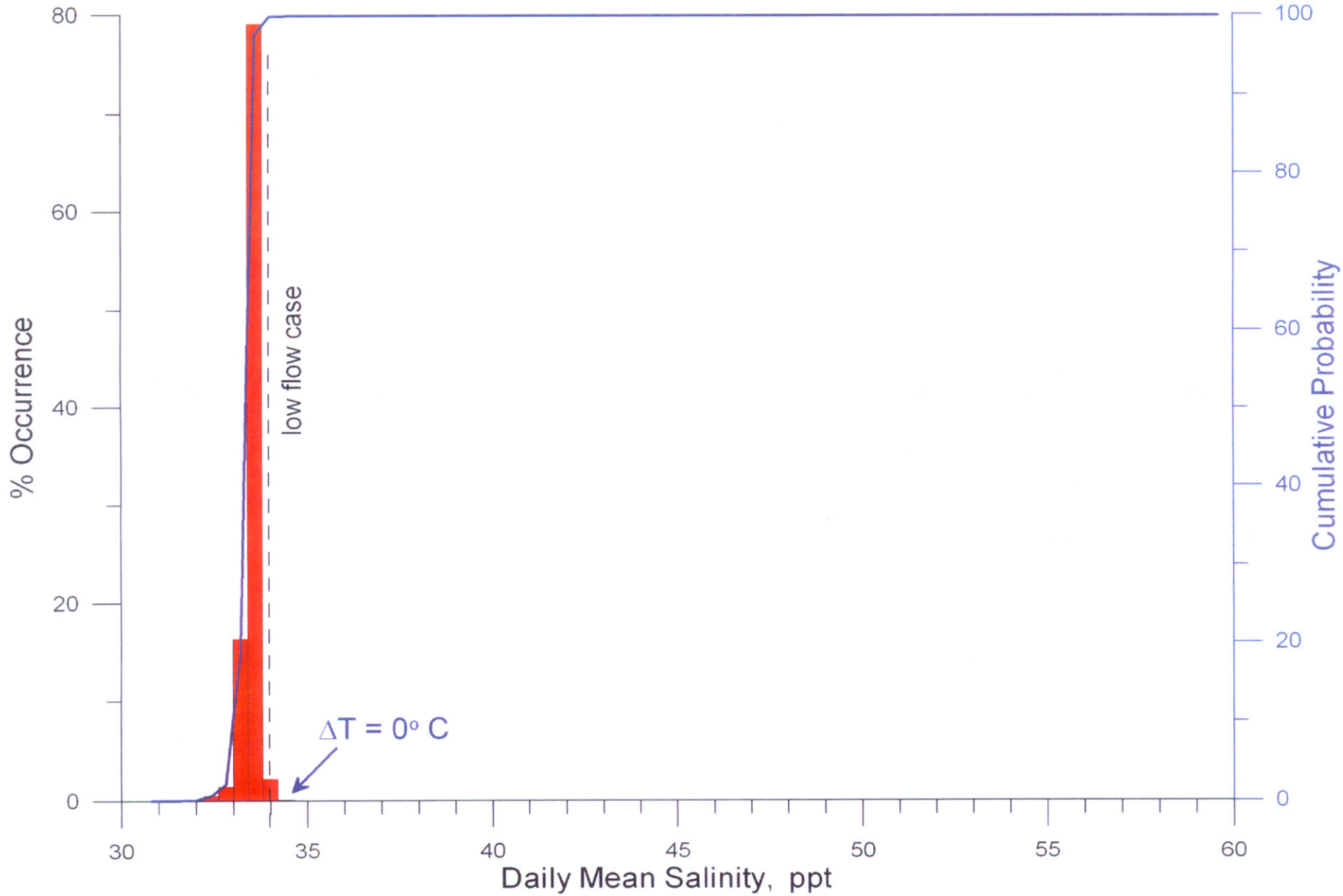

Figure 5.15. Histogram of daily maximum salinity at mid-depth and 2000 meters from the AES outfall for desalination production rate of 50 mgd. Percent occurrence based on historic observations of ocean mixing and water mass mass properties, and AES daily plant flow rates, 1980-2000.

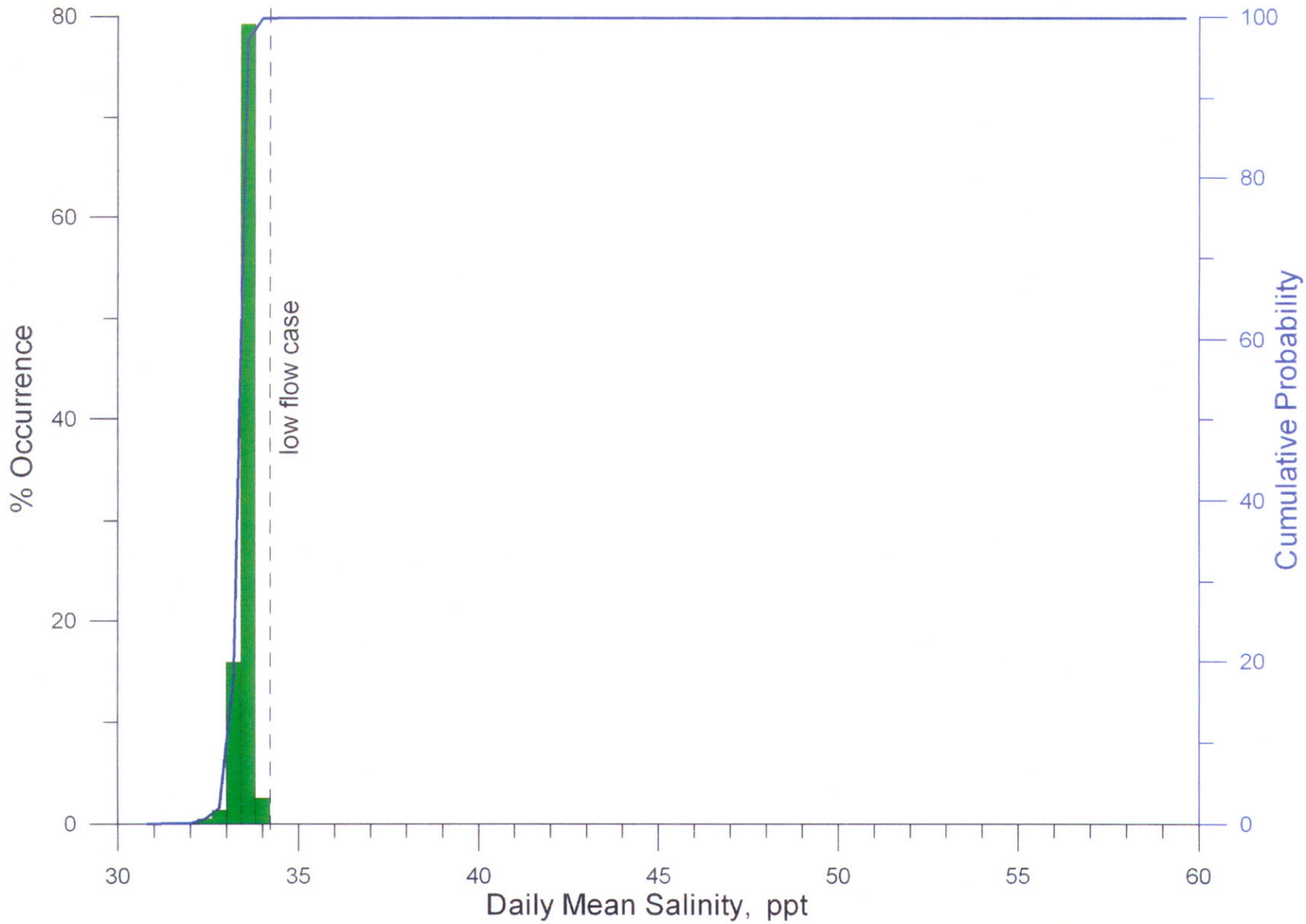

Figure 5.16. Histogram of daily maximum salinity at the bottom and 2000 meters from the AES outfall for desalination production rate of 50 mgd. Percent occurrence based on historic observations of ocean mixing and water mass mass properties, and AES daily plant flow rates, 1980-2000.

dilute the 50 mgd of concentrated sea water from the desalination plant. This historic 2 mode operational pattern introduced a bimodal statistical pattern into the model results of this study and a probable bias for persistence of low plant flow rate conditions.

The results of this study are summarized in Table 7. Entries are given for the characteristic daily maximum salinities that can be expected for various distances away from the out fall extending as far as 2,000 meters (1.2 miles). Characteristic salinities were identified in the peaks of the probability density distributions (histograms); and two well defined peaks were identified with the two predominant operational modes of the generating station giving a bi-modal distribution. Outcomes for those peaks in the bi-modal probability density distribution are indicated in red in Table 7. One peak (low-flow rate peak) was attributed to the operation of only one generating unit, and give the highest salinities in the discharge plume. These are listed in the second and third columns of Table 7. The third and fourth columns of Table 7 give the outcomes for the other peak in the probability density distribution (mid-flow rate peak) resulting from operation of two generating units. The salinities of the low-flow rate peak start out at 55 ppt in the water column above the outfall and fall off to 39 ppt at 150 meters away, accounting for between 42% and 48% of the modeled outcomes. On the sea floor, the low-flow rate operational condition (one generating unit) produces salinities that typically range from 47.5 ppt at the foot of the outfall to 37.0 ppt at 150 meters from the outfall with the same recurrence rates as found in the water column. During times when two generating units(or more) were operated (mid-flow rate peak), salinities varied in the water column from 41.6 ppt at the outfall to 35.2 ppt at 150 meters away with a recurrence rate of 52% to 58%.

Table 7. Generalized Salinity Plume from 7,523 outcomes, 1980- July 2000

Distance from Outfall (m)	One Generating Unit[a]		Two Generating Units	
	Characteristic Salinity (ppt)	Recurrence Rate (%)	Characteristic Salinity (ppt)	Recurrence Rate (%)
0 Mid-depth	55.2	48%	41.6	52%
0 Bottom	47.5	48%	38.6	52%
50 Mid-depth	45.4	48%	37.4	52%
50 Bottom	40.0	48%	36.0	52%
100 Mid-depth	43.0	47%	36.6	53%
100 Bottom	37.8	43%	35.0	57%
150 Mid-depth	39.0	42%	35.2	58%
150 Bottom	37.0	42%	34.8	58%
300 Mid-depth	36.2	40%	34.6	60%
300 Bottom	36.0	40%	34.6	60%
500 Mid-depth	35.0	25%	34.0	75%
500 Bottom	35.2	30%	34.4	70%
1000 Mid-depth	34.0	18%	33.6	82%
1000 Bottom	34.2	18%	33.6	82%
2000 Mid-depth	33.5	100%	33.5	100%
2000 Bottom	33.5	100%	33.5	100%

[a] includes cold water discharges, $\Delta T = 0\ ^{o}C$

[b] red indicates values associated with bimodal probability density distributions

[c] green indicates values associated with uni-modal probability density distributions

On the sea floor, 2 generating unit operation (mid-flow rates) causes salinity to range from 38.6 ppt at the foot of the outfall to 34.8 ppt at 150 meters away with the same recurrence rate as for the water column.

Beyond 150 meters from the outfall, the probability density distribution for the discharge plume salinities no longer exhibits bi-modal character. Because the salinity contrast with the ambient water is greater for the low-flow rate peak, it becomes smeared by higher mixing rates promoted along stronger concentration gradients and it merges with the mid-flow rate peak in the distribution to form an asymmetric uni-modal distribution. The characteristics of this distribution are mid-flow rate peak at lower salinities with a low-flow rate shoulder extending into higher salinity ranges. The outcomes that exhibit this uni-model probability density distribution are listed in green in Table 2. Salinities in the mid-flow rate peak of this distribution range from 34.6 ppt at 300 meters from the outfall and decay down to ambient ocean salinity at 2,000 meters from the outfall with a recurrence rate of 60% to 82% before reaching ambient ocean salinity levels. Salinities are only a fraction of a ppt greater on the bottom than in the water column over this range. For the low flow rate shoulder of the probability density distribution, salinites vary from 36.2 ppt 300 meters from the outfall to ambient salinity 2000 meters away, with recurrence rate of 40% down to 18% before reaching ambient ocean salinity levels.

The bi-modal statistical bias imprinted on the model results by the historical plant flow rates throughout the re-fitting period appears to exhibit itself only in the nearfield of the outfall. The recurrence pattern of two distinct outcomes of approximately equal likelihood, one of high salinity and the other of more moderate salinity, is only apparent in the inner and outer core of the discharge plume,

extending out to about 150 meters from the out fall. This is an area of about 17.5 acres. In the salt wedge portion of the plume from 500 meters out and beyond, operational patterns do not appear to alter the results by more than about 1 ppt, with salinities occurring between 34 ppt and 35 ppt or less regardless of historic operational tendencies. In the intermediate zone between 150 and 500 meters from the outfall, there is some residual effect of operational pattern. Here operational patterns can mean the difference between 36 ppt or about 34.5 ppt, that is the difference between exceeding the upper limit of the natural ocean salinity range for this region or not. In spite of the historical patterns there were no outcomes involving generation of electrical power that resulted in discharge salinities exceeding those of the Section 4 low flow case scenario. Only for the particular non-generating scenario of "Zero Delt-T" ($\Delta T = 0$ °C) did higher salinites occur, and these exceeded the Section low flow case by no more than 1 ppt and accounted for only 1% to 6% of all possible outcomes.

Now that re-powering of the AES Huntington Beach generating station is complete, it is sensible to expect that it will be operated at higher production levels than those observed for the late 1980's and throughout the 90's. This is evident from the plant flow rate history for the post re-fit period, from 2002 to July of 2003 as shown in Figure 5.17. Average flow rates of the plant during this period was 265 mgd and the operational pattern involved a balanced proportion of all four generating units. This most recent plant flow rate average exceeds the average for the model simulation period when the plant operated close to the Section 4 low flow case conditions throughout the 1990's. Consequently the persistence analysis of Sections 5 A-H was likely biased towards a low- flow rate operational pattern that may not be representative of the future conditions in which

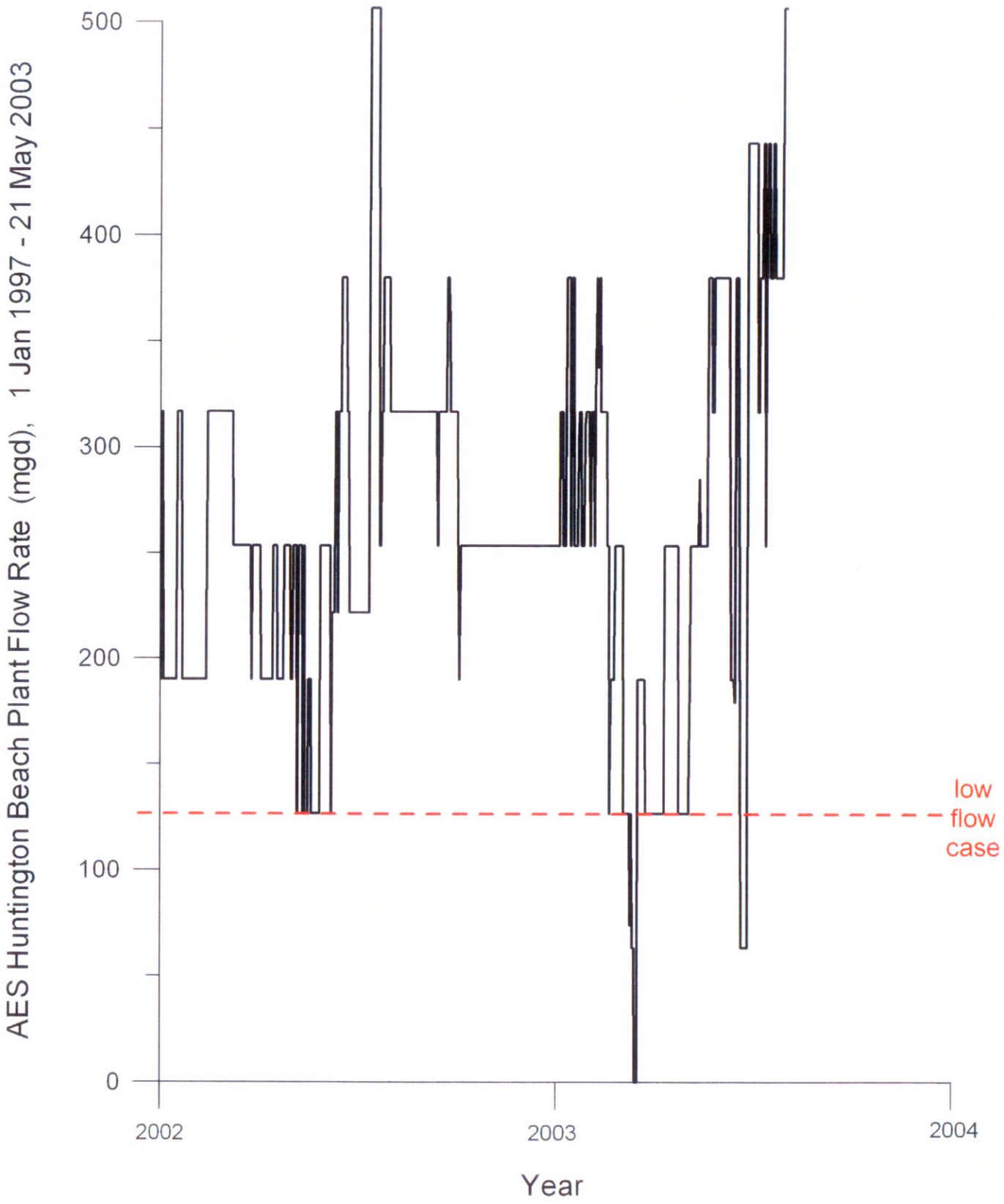

Figure 5.17. Most recent history of AES Power Plant flow rate 1 January 2002 - 30 July 2003 (19 Months). Value for "worst case" modeling scenario shown in red.

the desalination plant is built. This bias will tend to over-estimate the intensity and persistence of the saline anomalies induced by the desalination plant, but should also provide a more cautious assessment of potential saline impacts to the marine environment. To prove this hypothesis, we repeat the long-term analysis methodology on the 7 controlling variables for the post re-powering period, 2 January 2002 - 30 July 2003 as plotted in Figures 5.18 and 5.19. The results are summarized in Table 8 and the histogram solution set is presented in Figures 5.20 through 5.34. Inspection of the end-of pipe salinities in Figure 5.20 shows that the low flow rate peak at 55 ppt is greatly reduced and represents only about 5% of the 578 daily outcomes in the post re-powering period. Even within 50 meters of the outfall (Figures 5.21 and 5.22) the histogram distribution is predominantly unimodal and centered on 35 ppt with 92% of the outcomes giving salinities elevated less than the 10% above ambient. Beyond 150 meters away from the outfall, no outcomes from the 7 controlling variables during the post re-powering period give rise to salinities exceeding 40 ppt anywhere in the water column or along the seabed. Furthermore, no outcomes at any distance from the outfall during post re-powering conditions reach give salinities as high as the low flow case events evaluated in Section 4. Thus, the operation of a 50 mgd desalination plant at AES Huntington Beach is unlikely to ever match or exceed the low flow case outcomes during the foreseeable future.

Table 8. Generalized Salinity Plume from 578 outcomes, January 02- July 03

Distance from Outfall (m)	Low Flow Rate Condition [a]		Nominal Flow Rate Condition	
	Characteristic Salinity (ppt)	Recurrence Rate (%)	Characteristic Salinity (ppt)	Recurrence Rate (%)
0 Mid-depth	55.2	9%	43.0	91%
0 Bottom	47.5	9%	39.0	91%
50 Mid-depth	45.4	9%	38.0	91%
50 Bottom	40.0	9%	35.0	91%
100 Mid-depth	42.8	8%	37.4	92%
100 Bottom	37.8	6%	35.6	94%
150 Mid-depth	38.0	6%	35.4	94%
150 Bottom	37.2	6%	35.2	94%
300 Mid-depth	36.0	3%	34.6	97%
300 Bottom	36.0	3%	34.6	97%
500 Mid-depth	35.0	1%	34.0	99%
500 Bottom	35.2	1%	34.2	99%
1000 Mid-depth	33.6	100%	33.6	100%
1000 Bottom	33.8	100%	33.8	100%
2000 Mid-depth	33.5	100%	33.5	100%
2000 Bottom	33.5	100%	33.5	100%

[a] includes all operating conditions pumping 126.7 mgd or less

[b] red indicates values associated with bimodal probability density distributions

[c] green indicates values associated with uni-modal probability density distributions

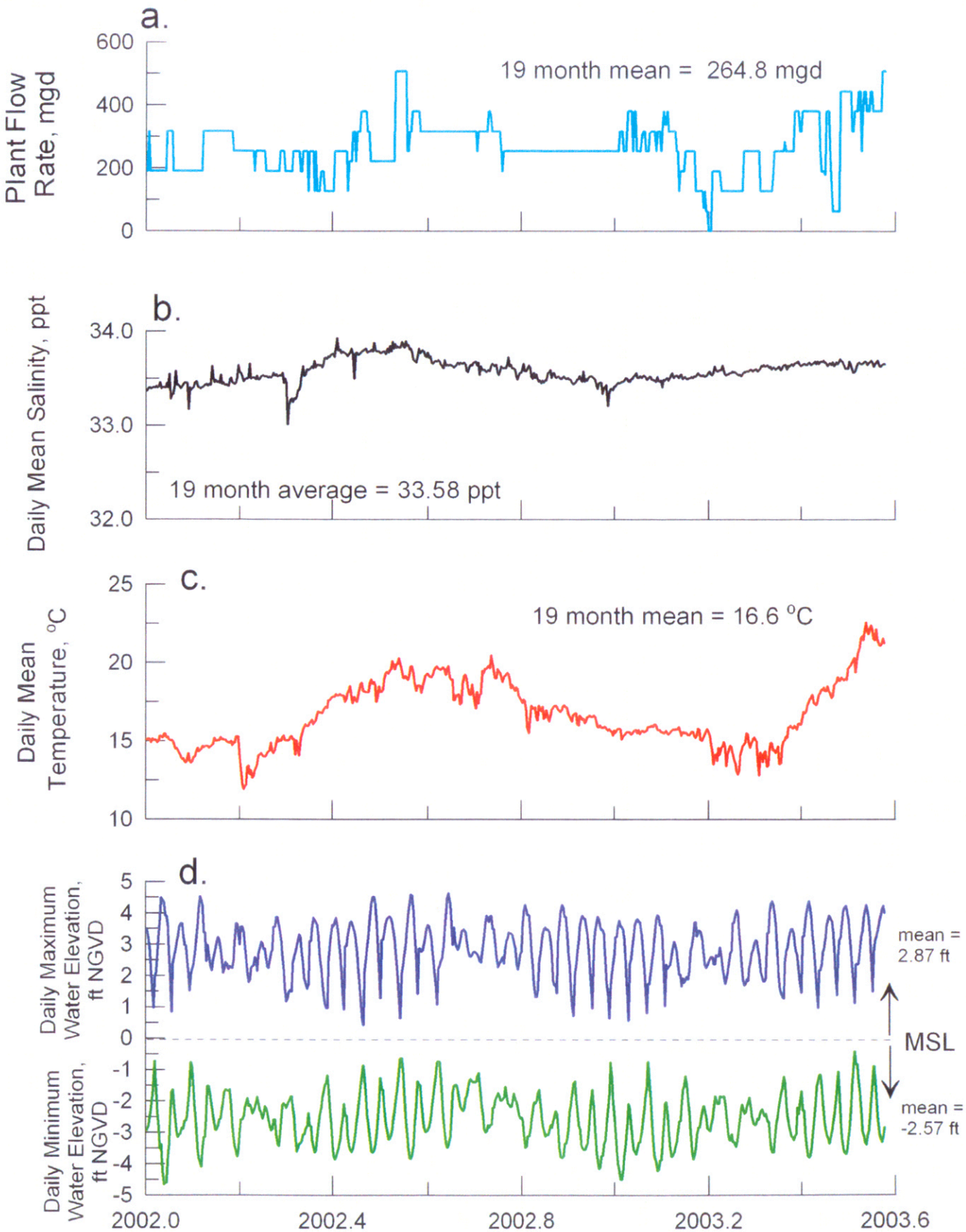

Figure 5.18. Controlling boundary condition variables for the post re-powering period of AES Huntington Beach, Jan 2, 2002 - July 30, 2003. a) plant flow rate b) daily mean salinity, c) daily mean temperature, and d) daily high and low water elevations. [data from MBC, 2002-03; CDIP, 2002-03; SIO, 2002-03]

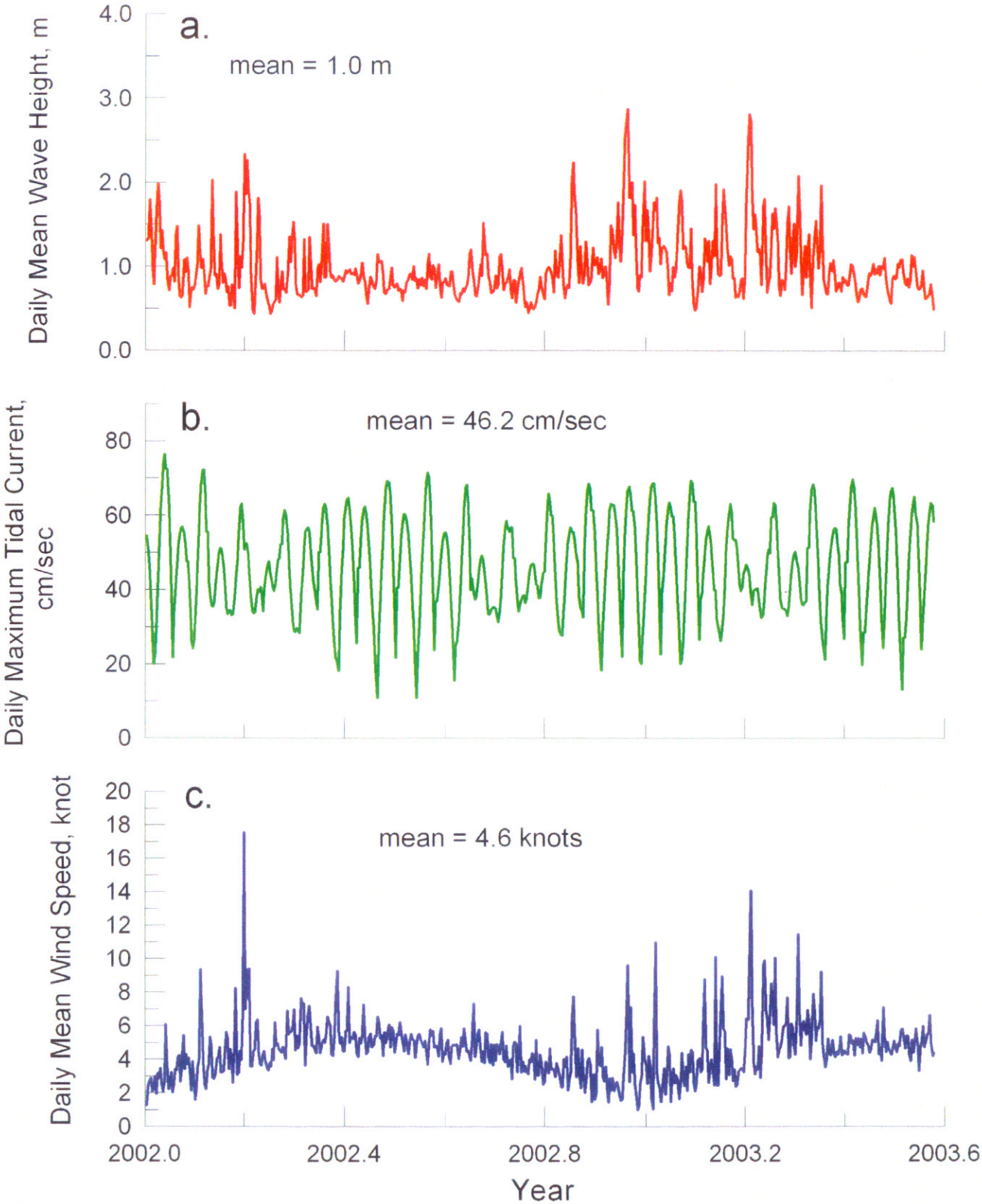

Figure 5.19. Controlling forcing function variables for the post re-powering period of AES Huntington Beach, Jan 1, 2002 - July 30, 2003. a) wave height; b) tidal currents; c) daily mean wind speed; [data from MBC, 2002-03; CDIP, 2002-03; UCAR, 2002-03]

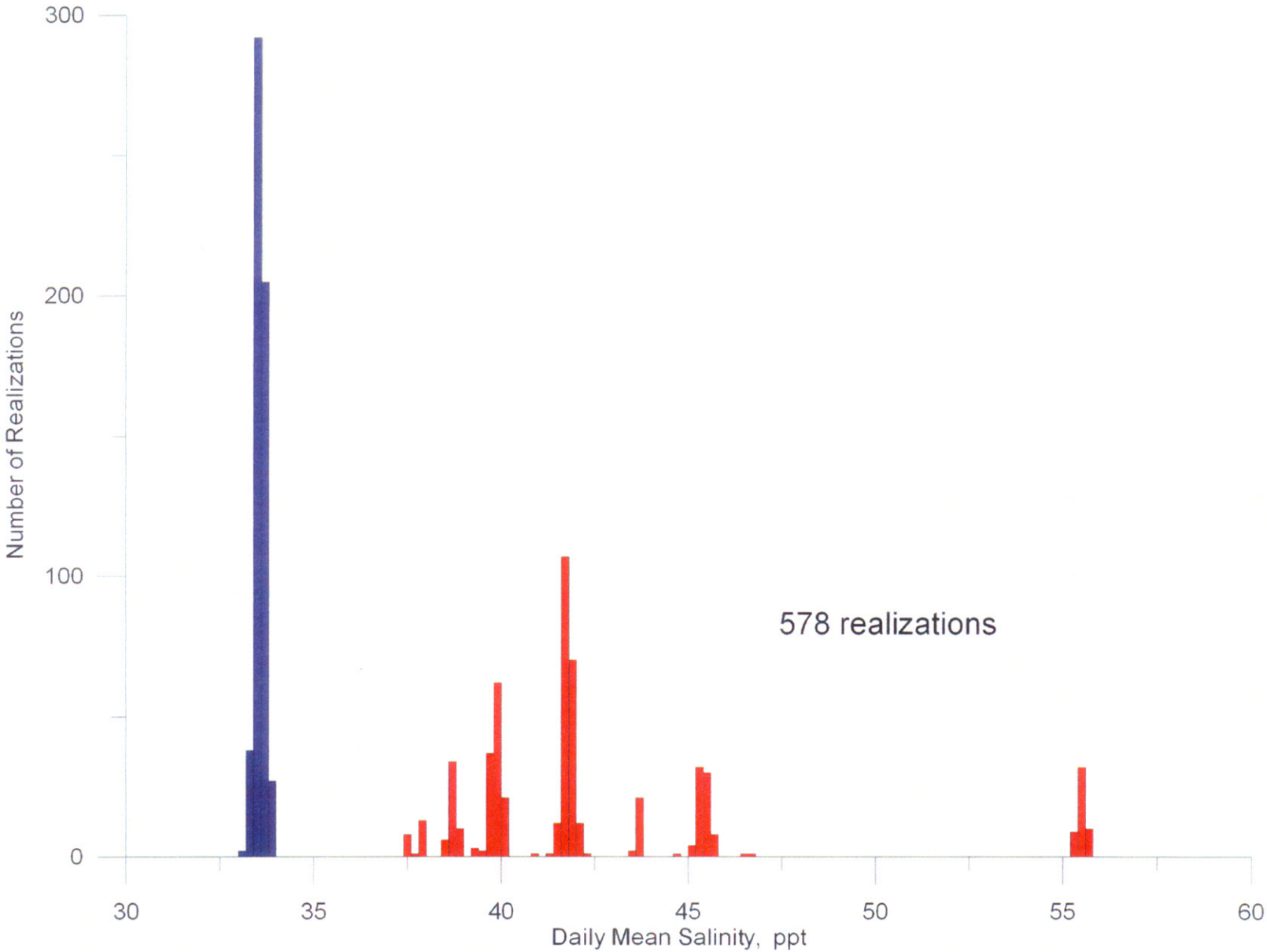

Figure 5.20. Histogram of daily mean salinity for the post re-powering period based on historic observations and AES daily plant flow rates, 1 Jan 2002-30 July 2003. Ocean salinity off Huntington Beach (blue) and end-of-pipe combined discharge salinity for desalination plant producing at 50 mgd (red).

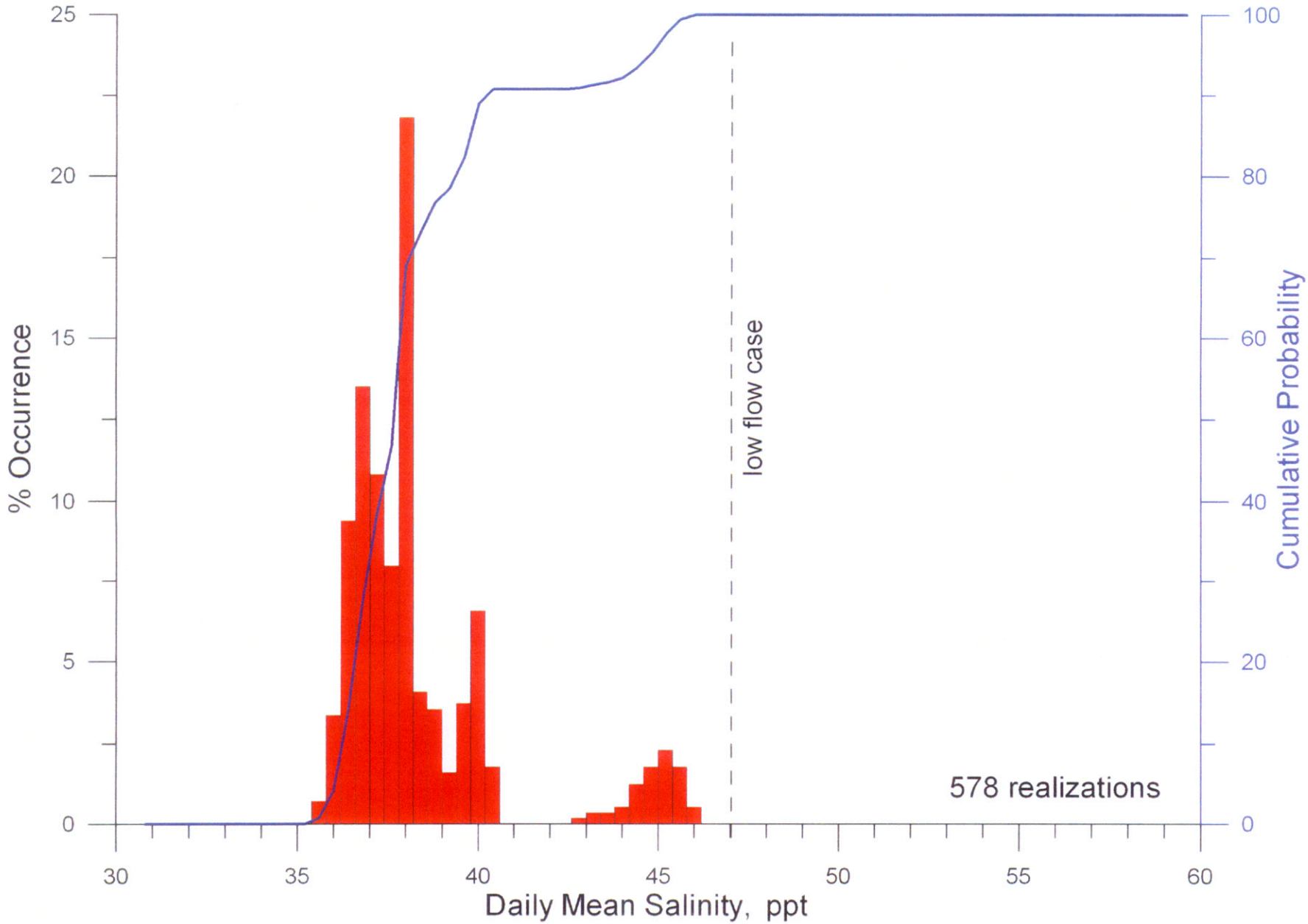

Figure 5.21. Histogram of daily maximum salinity at mid-depth and 50 meters from the AES outfall for desalination production rate of 50 mgd. Percent occurrence based on historic observations of ocean mixing and water mass mass properties, and AES daily plant flow rates for the post re-powering period, 1 Jan 2002 - 30 July 2003.

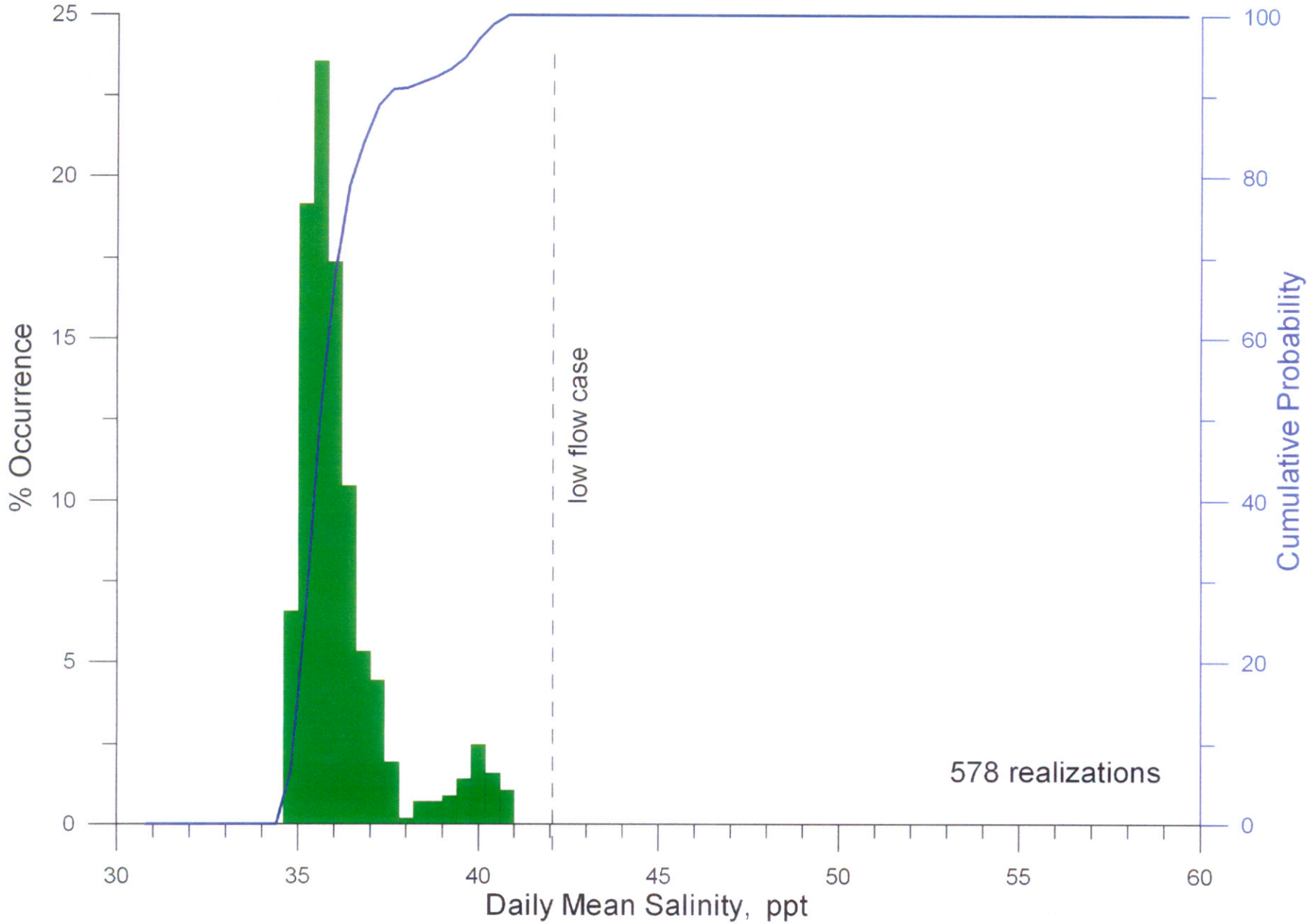

Figure 5.22. Histogram of daily maximum salinity at the bottom and 50 meters from the AES outfall for desalination production rate of 50 mgd. Percent occurrence based on historic observations of ocean mixing and water mass mass properties, and AES daily plant flow rates for the post re-powering period, 1 Jan 2002 - 30 July 2003.

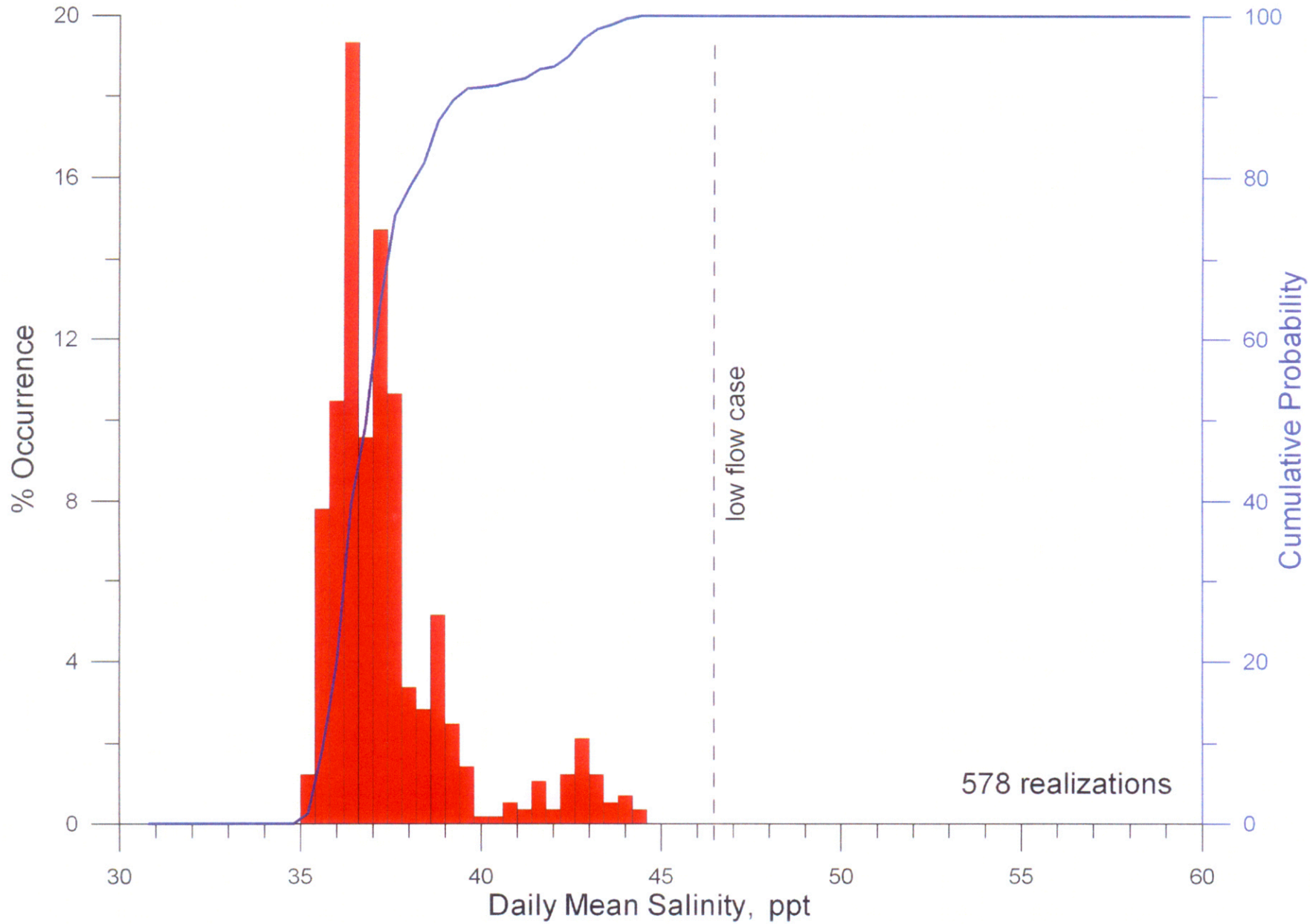

Figure 5.23. Histogram of daily maximum salinity at mid-depth and 100 meters from the AES outfall for desalination production rate of 50 mgd. Percent occurrence based on historic observations of ocean mixing and water mass mass properties, and AES daily plant flow rates for the post re-powering period, 1 Jan 2002 - 30 July 2003.

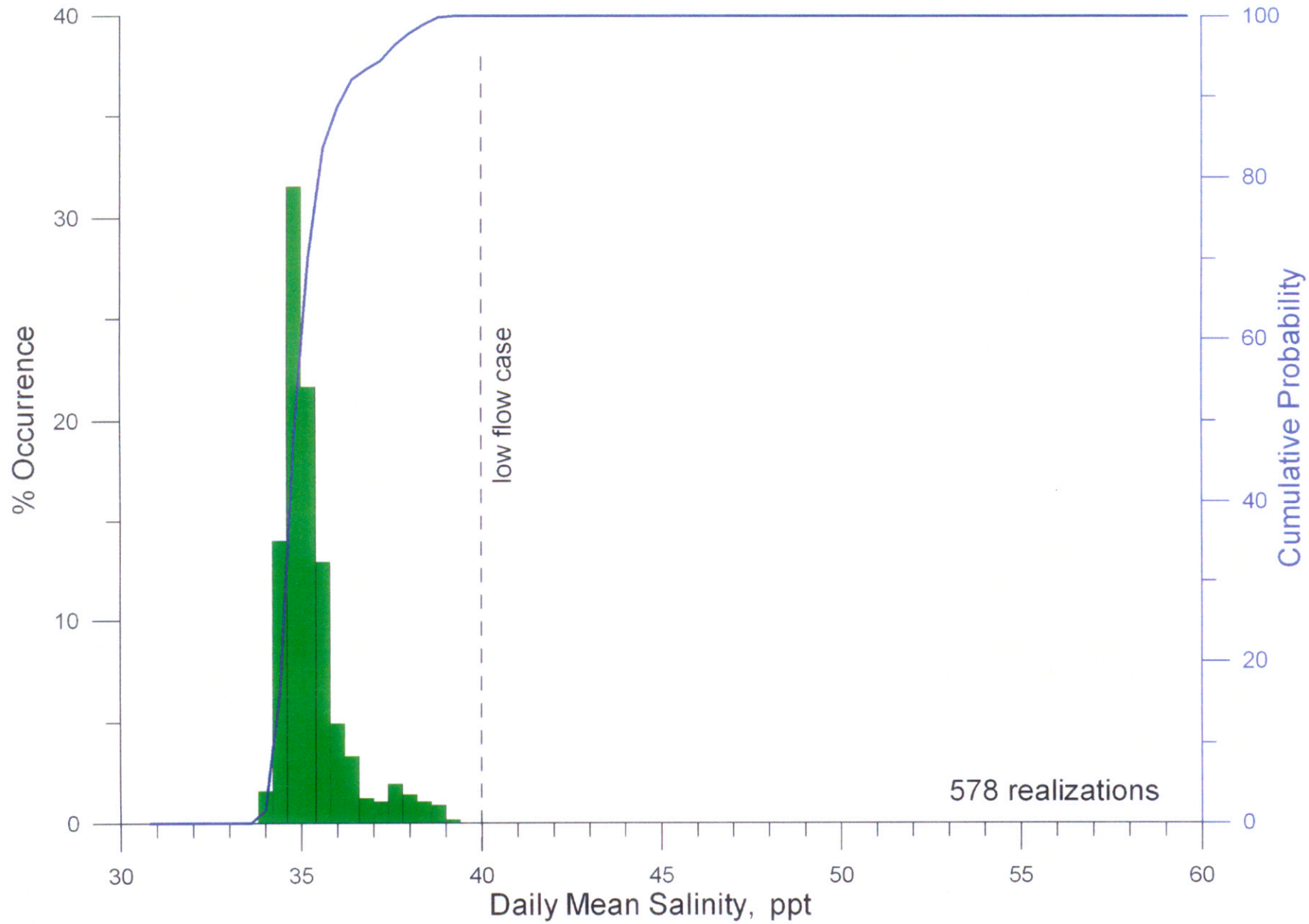

Figure 5.24. Histogram of daily maximum salinity at the bottom and 100 meters from the AES outfall for desalination production rate of 50 mgd. Percent occurrence based on historic observations of ocean mixing and water mass mass properties, and AES daily plant flow rates for the post re-powering period, 1 Jan 2002 - 30 July 2003.

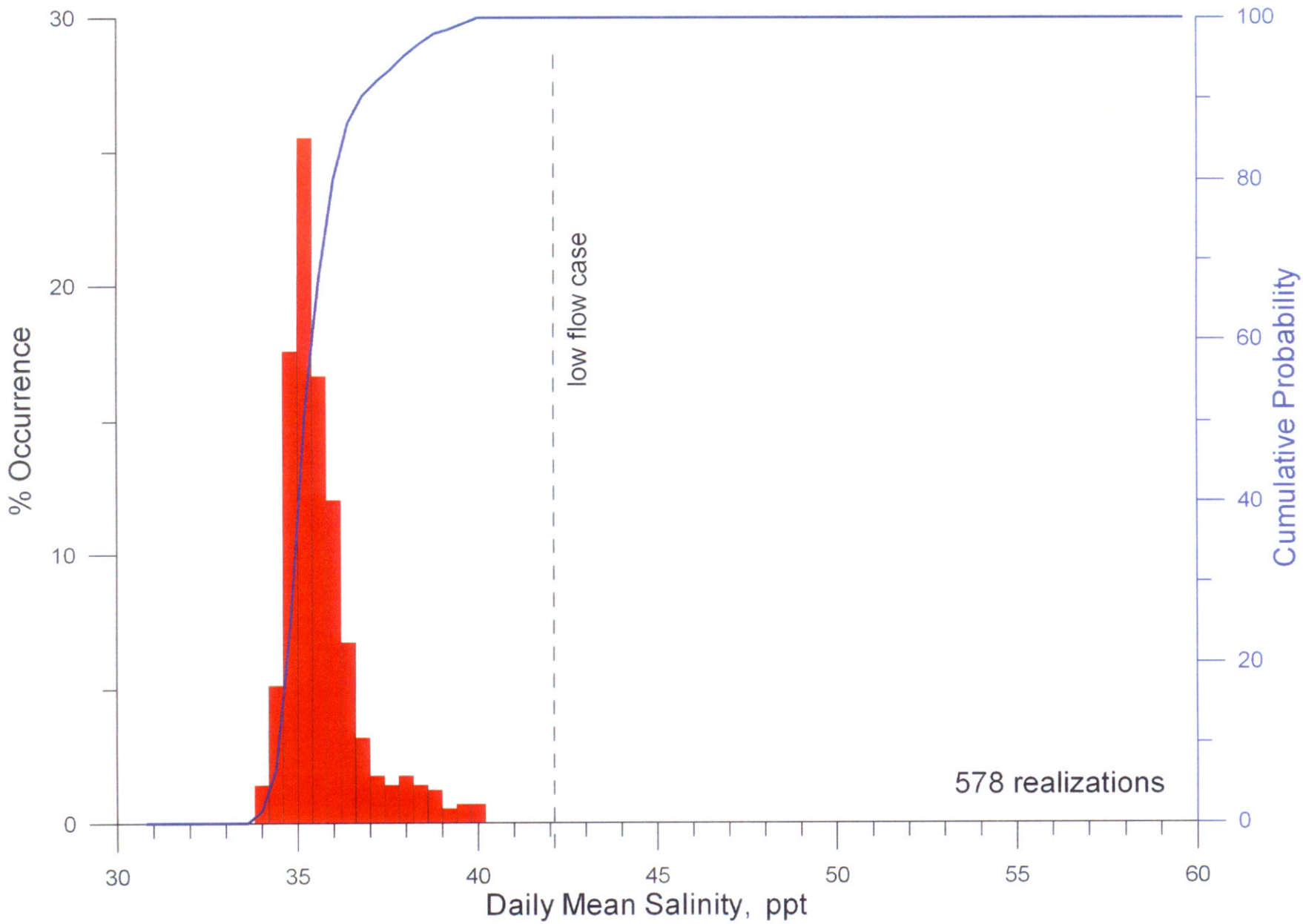

Figure 5.25. Histogram of daily maximum salinity at mid-depth and 150 meters from the AES outfall for desalination production rate of 50 mgd. Percent occurrence based on historic observations of ocean mixing and water mass mass properties, and AES daily plant flow rates for the post re-powering period, 1 Jan 2002 - 30 July 2003.

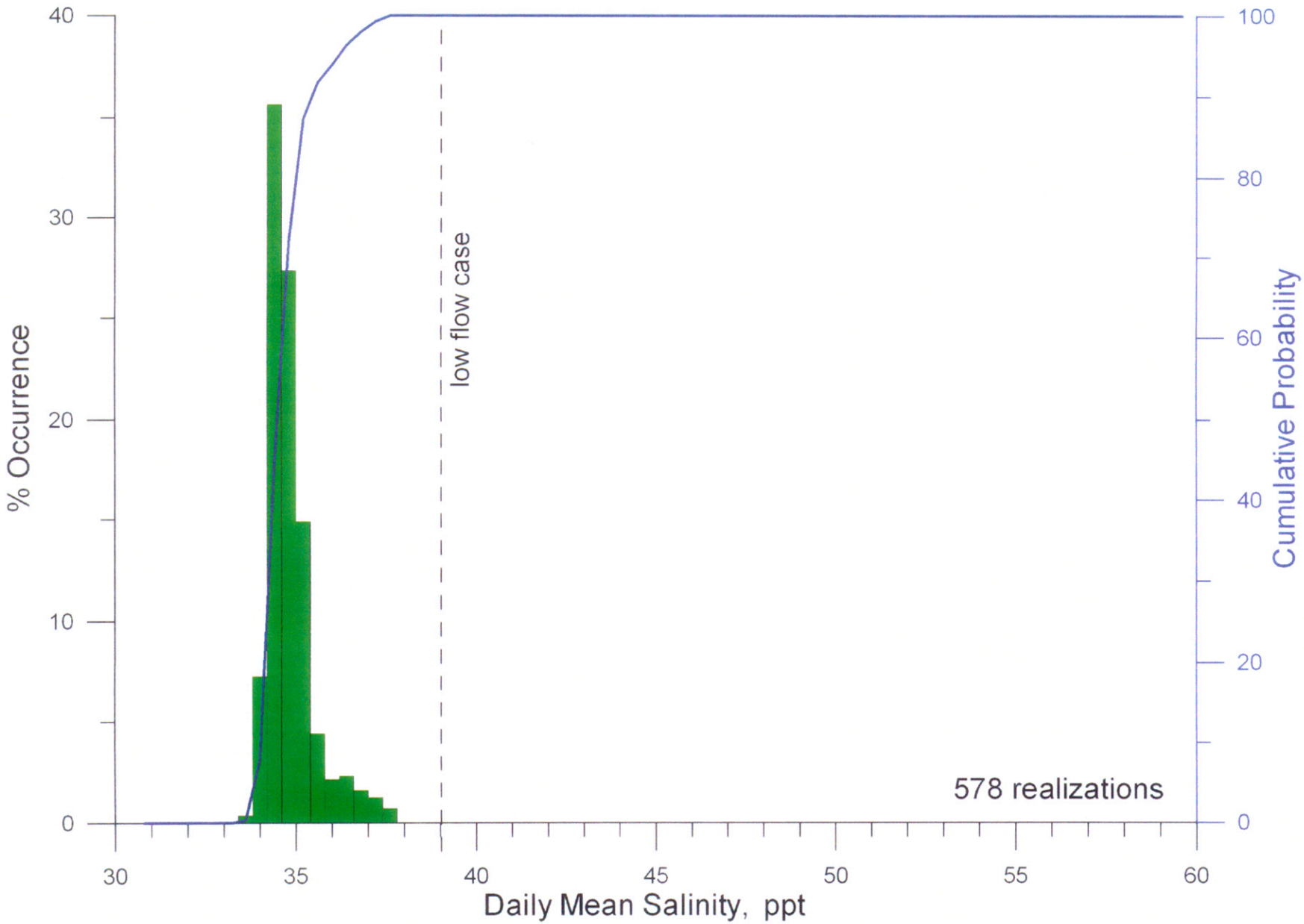

Figure 5.26. Histogram of daily maximum salinity at the bottom and 150 meters from the AES outfall for desalination production rate of 50 mgd. Percent occurrence based on historic observations of ocean mixing and water mass mass properties, and AES daily plant flow rates for the post re-powering period, 1 Jan 2002 - 30 July 2003.

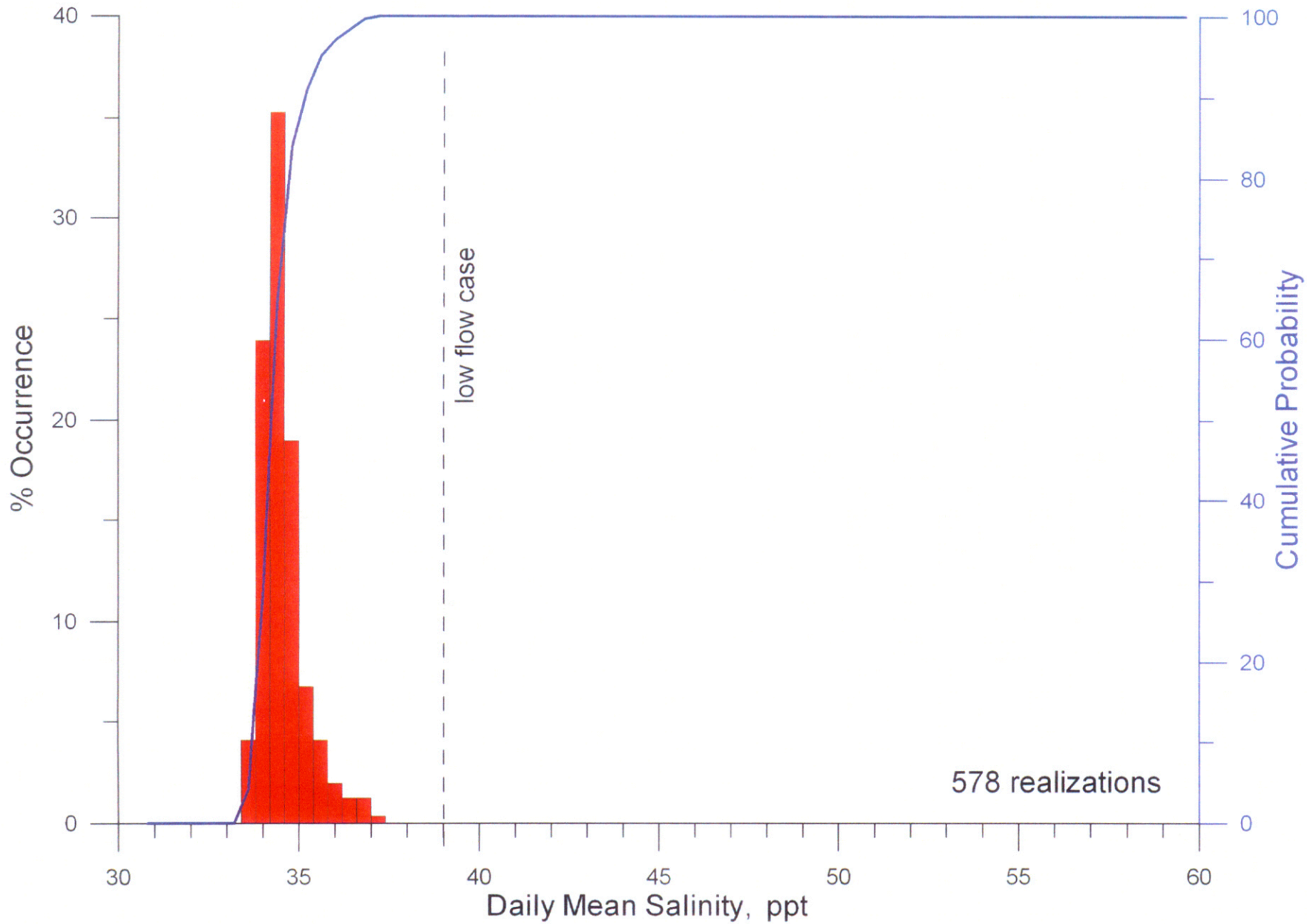

Figure 5.27. Histogram of daily maximum salinity at mid-depth and 300 meters from the AES outfall for desalination production rate of 50 mgd. Percent occurrence based on historic observations of ocean mixing and water mass mass properties, and AES daily plant flow rates for the post re-powering period, 1 Jan 2002 - 30 July 2003.

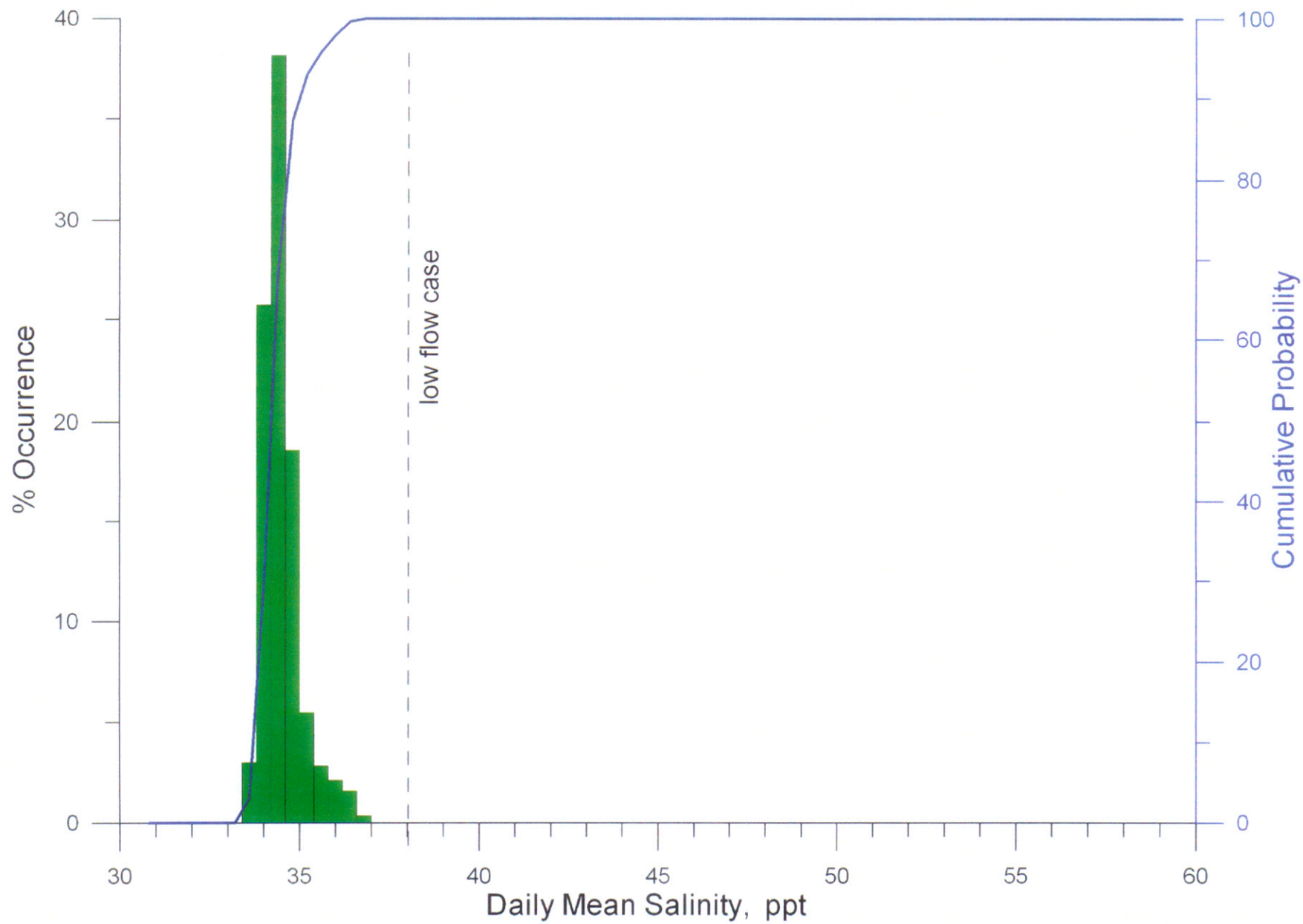

Figure 5.28. Histogram of daily maximum salinity at the bottom and 300 meters from the AES outfall for desalination production rate of 50 mgd. Percent occurrence based on historic observations of ocean mixing and water mass mass properties, and AES daily plant flow rates for the post re-powering period, 1 Jan 2002 - 30 July 2003.

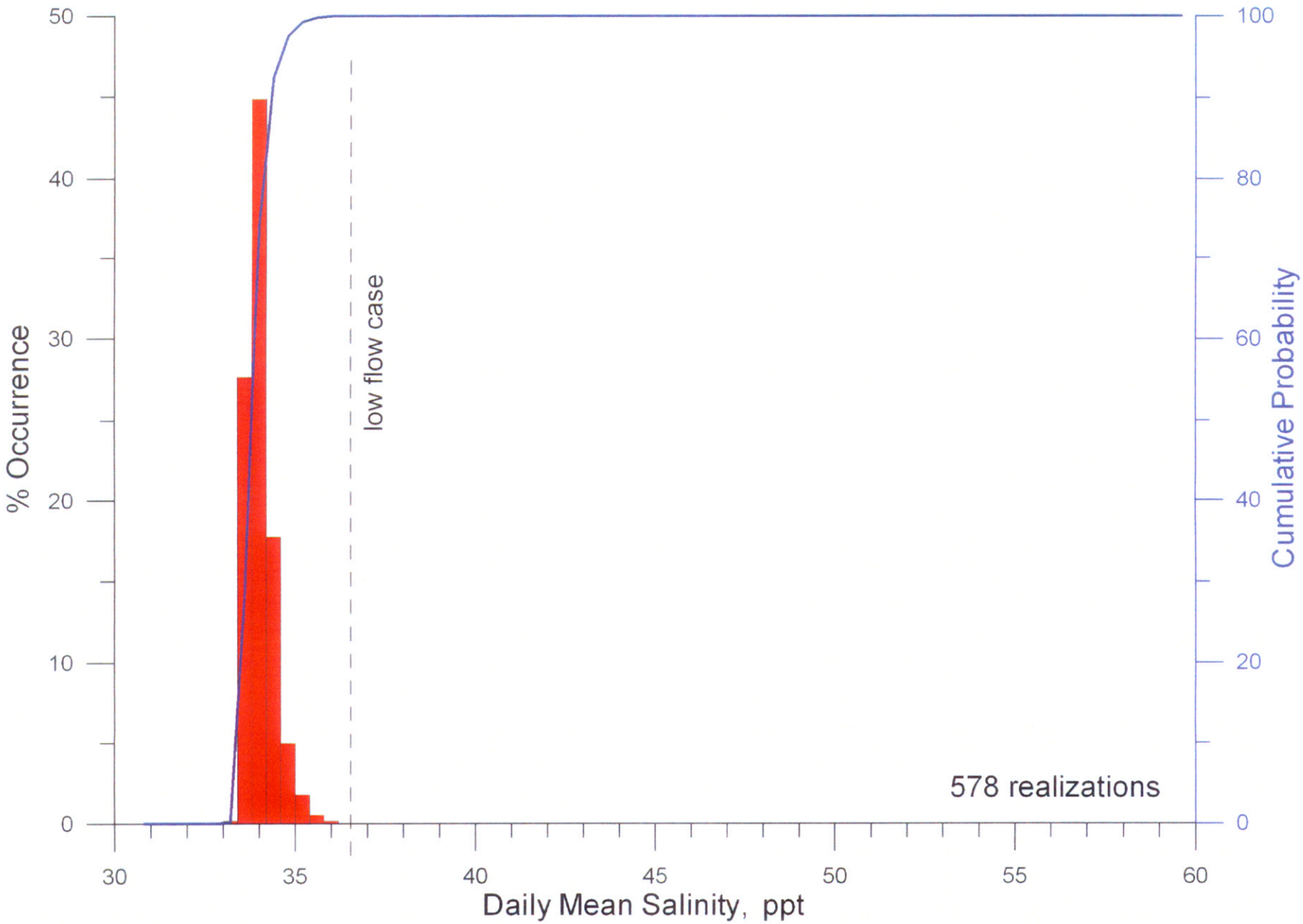

Figure 5.29. Histogram of daily maximum salinity at mid-depth and 500 meters from the AES outfall for desalination production rate of 50 mgd. Percent occurrence based on historic observations of ocean mixing and water mass mass properties, and AES daily plant flow rates for the post re-powering period, 1 Jan 2002 - 30 July 2003.

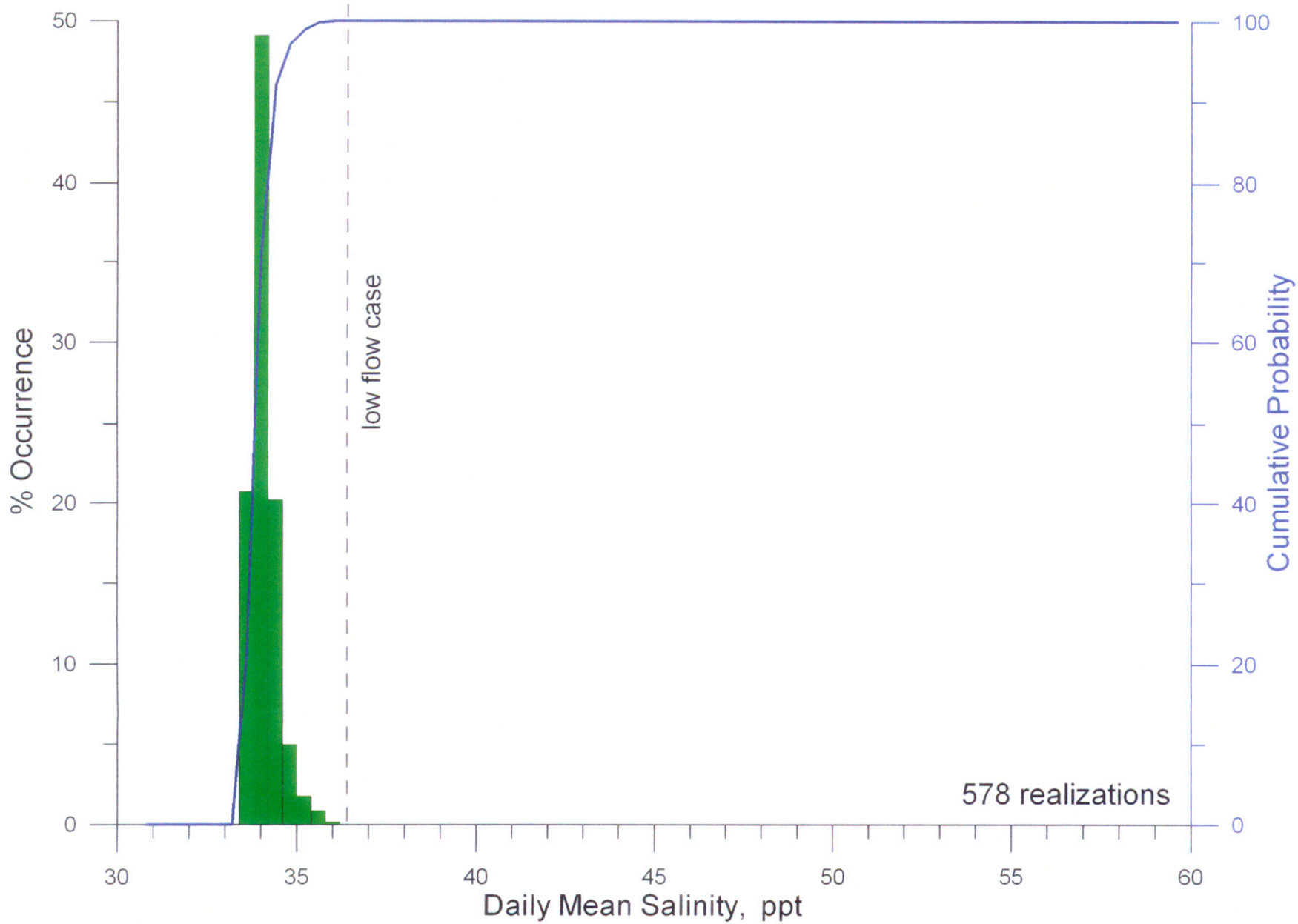

Figure 5.30. Histogram of daily maximum salinity at the bottom and 500 meters from the AES outfall for desalination production rate of 50 mgd. Percent occurrence based on historic observations of ocean mixing and water mass mass properties, and AES daily plant flow rates for the post re-powering period, 1 Jan 2002 - 30 July 2003.

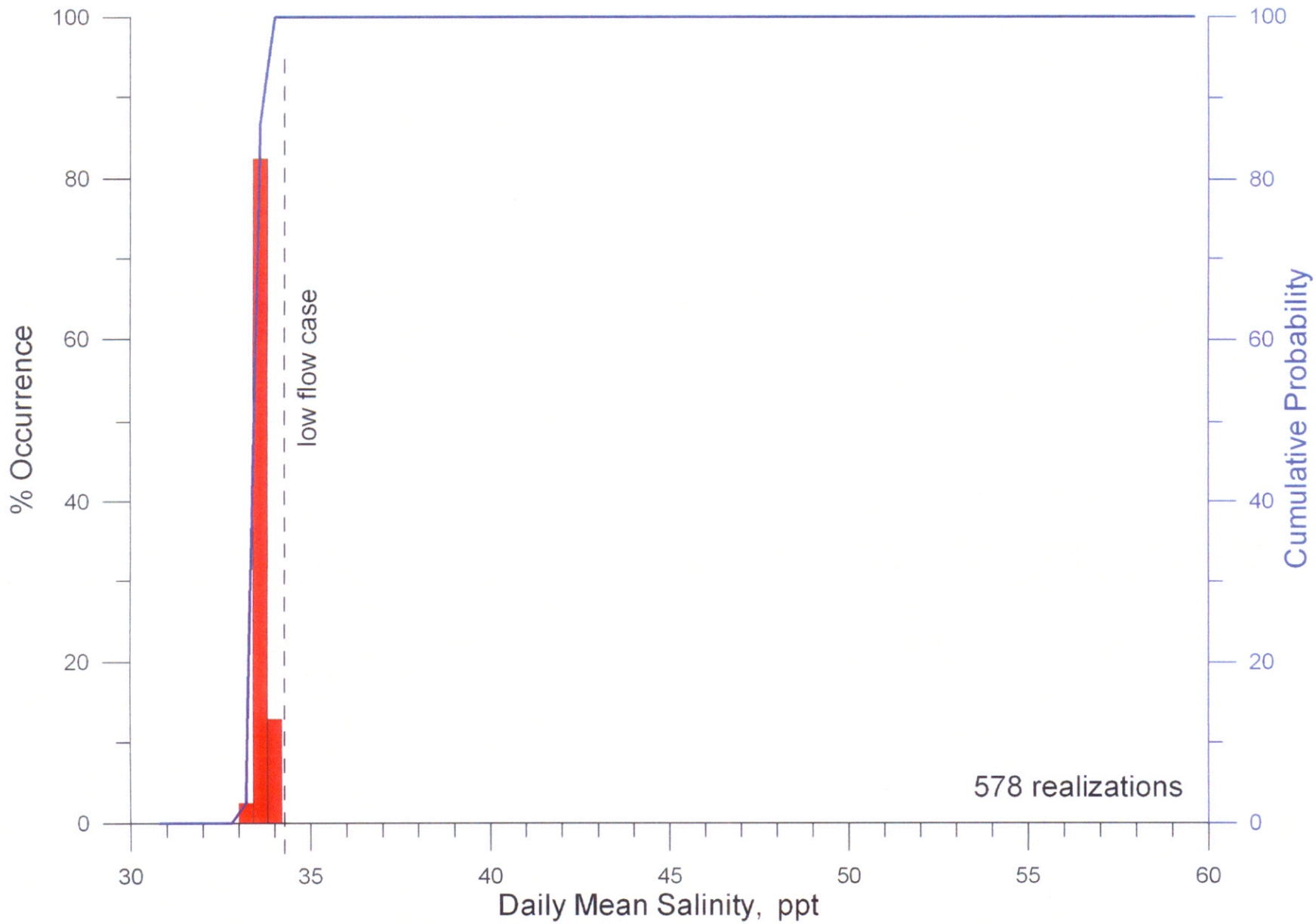

Figure 5.31. Histogram of daily maximum salinity at mid-depth and 1000 meters from the AES outfall for desalination production rate of 50 mgd. Percent occurrence based on historic observations of ocean mixing and water mass mass properties, and AES daily plant flow rates for the post re-powering period, 1 Jan 2002 - 30 July 2003.

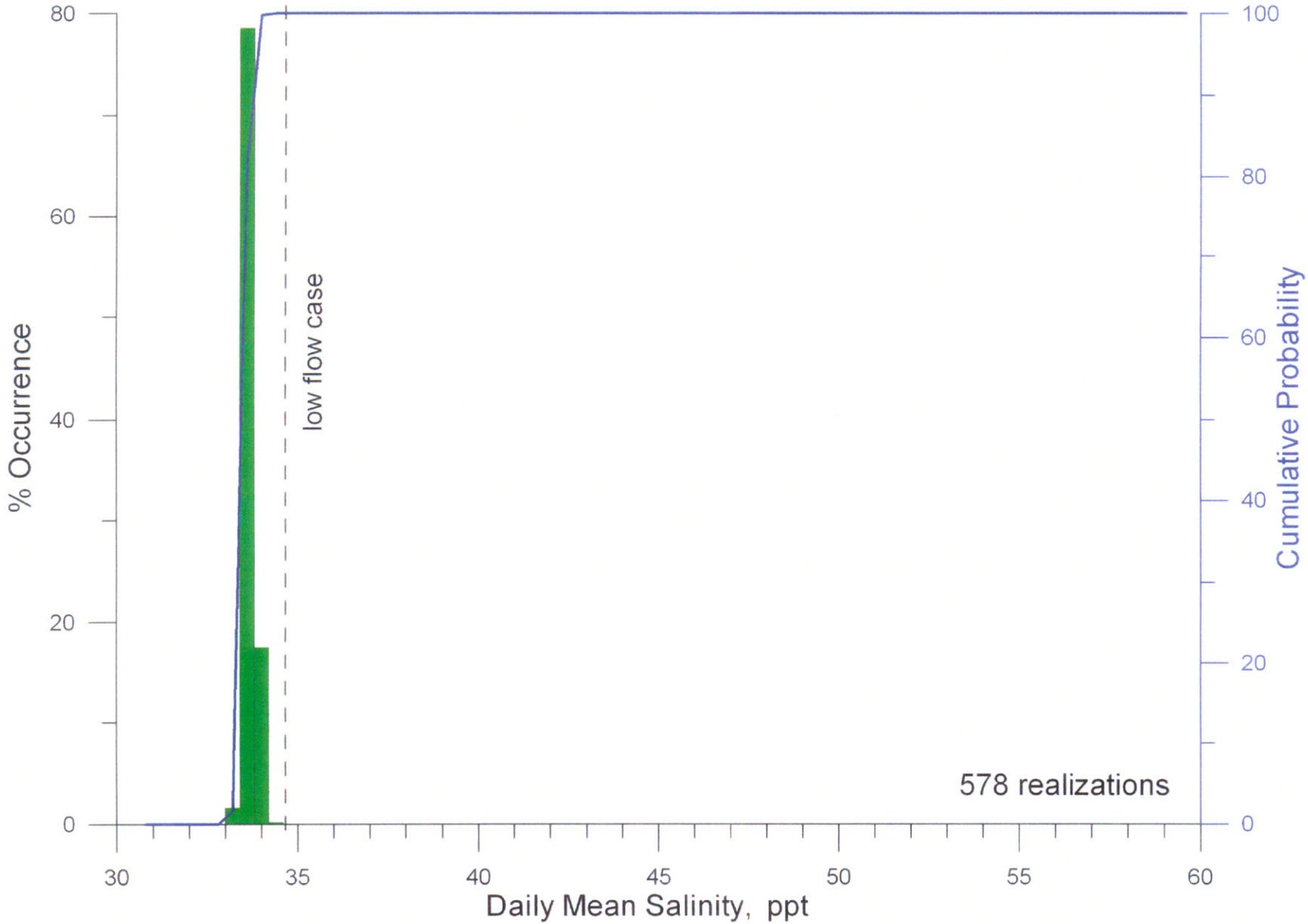

Figure 5.32. Histogram of daily maximum salinity at the bottom and 1000 meters from the AES outfall for desalination production rate of 50 mgd. Percent occurrence based on historic observations of ocean mixing and water mass mass properties, and AES daily plant flow rates for the post re-powering period, 1 Jan 2002 - 30 July 2003.

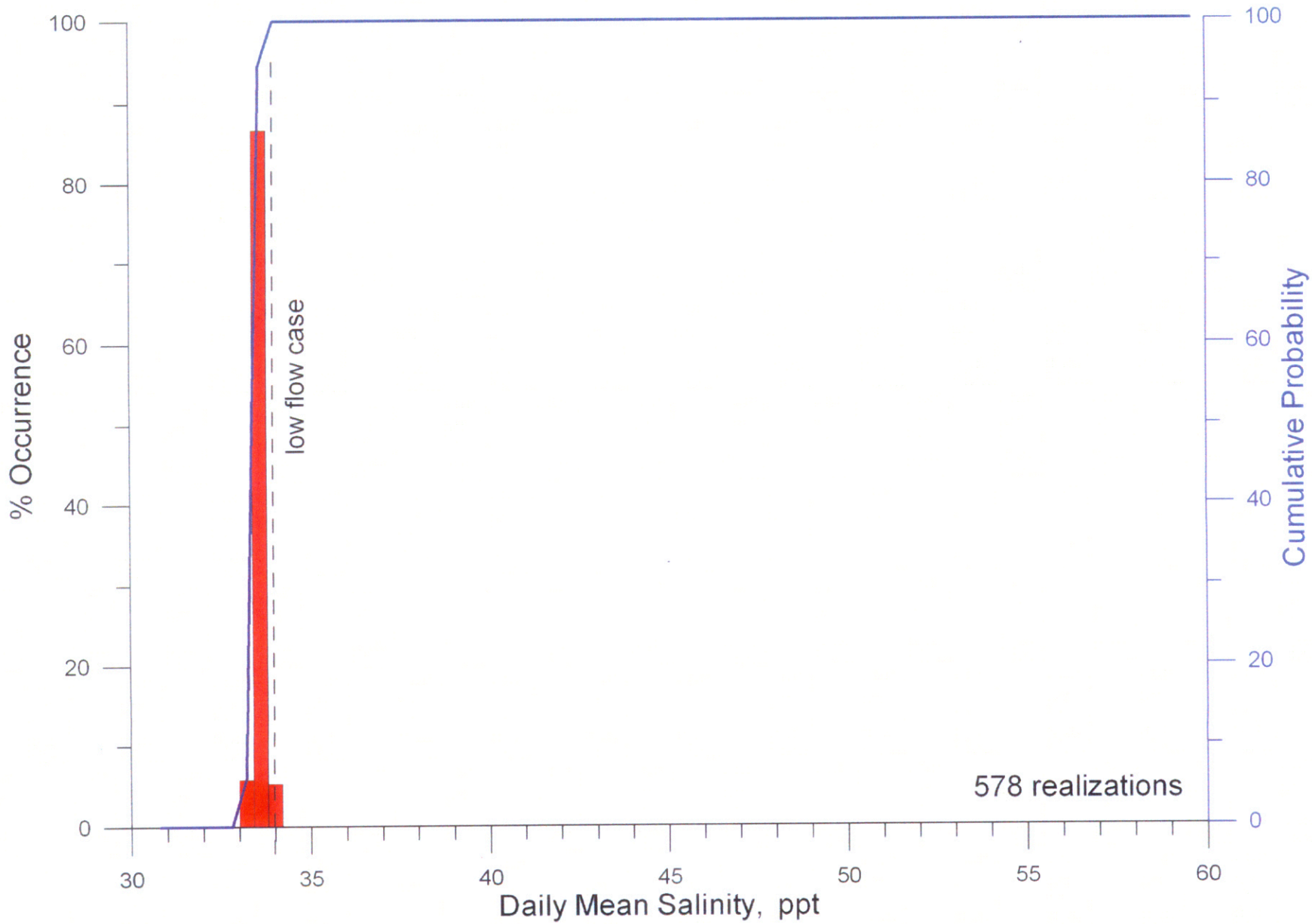

Figure 5.33. Histogram of daily maximum salinity at mid-depth and 2000 meters from the AES outfall for desalination production rate of 50 mgd. Percent occurrence based on historic observations of ocean mixing and water mass mass properties, and AES daily plant flow rates for the post re-powering period, 1 Jan 2002 - 30 July 2003.

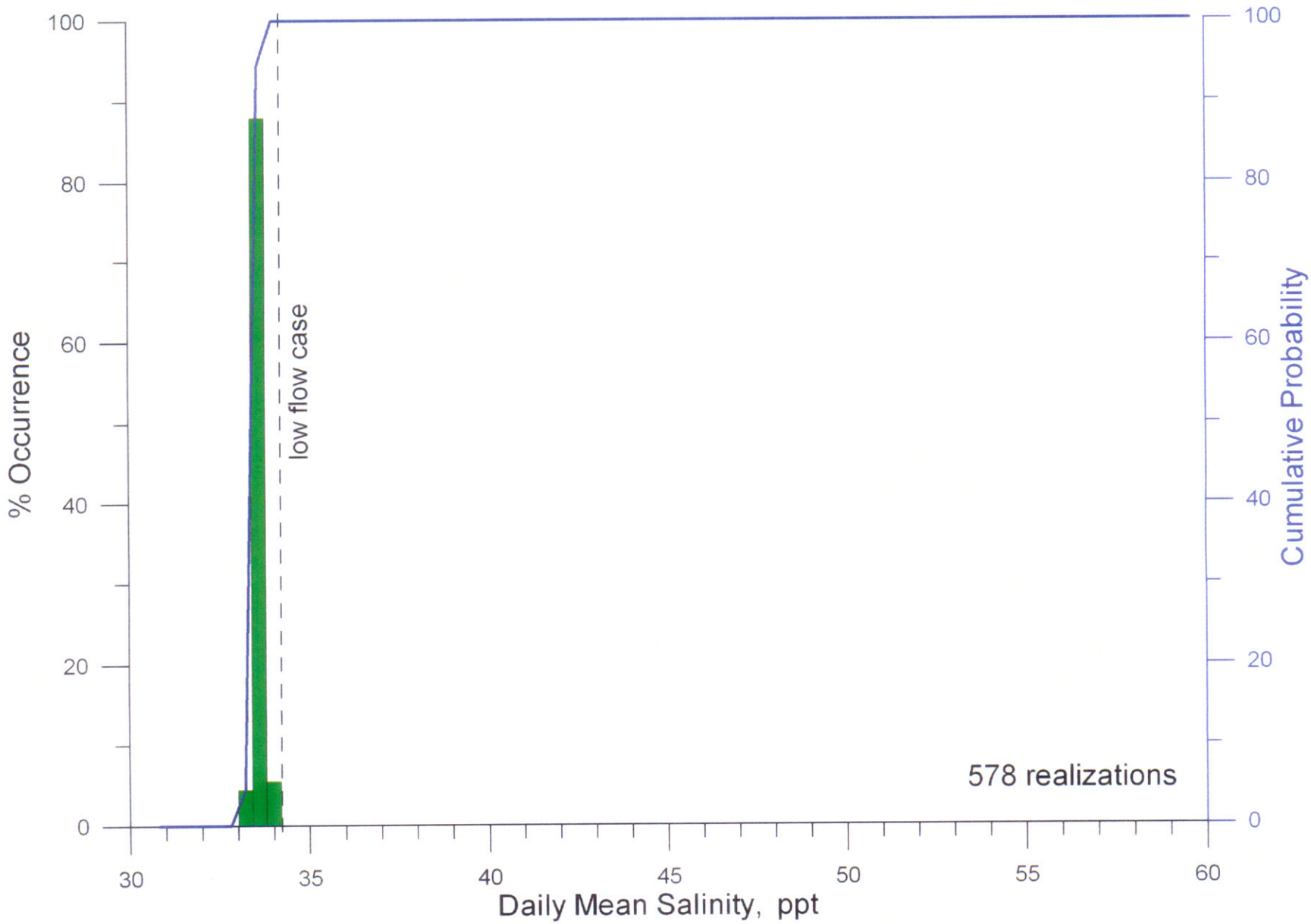

Figure 5.34. Histogram of daily maximum salinity at the bottom and 2000 meters from the AES outfall for desalination production rate of 50 mgd. Percent occurrence based on historic observations of ocean mixing and water mass mass properties, and AES daily plant flow rates for the post re-powering period, 1 Jan 2002 - 30 July 2003.